Development of Nanostructured DNA Aimed at Enhancing the Stability and Antigen-presenting Cell Targetability of CpG Oligodeoxynucleotide

（CpG オリゴデオキシヌクレオチドの安定性および抗原提示細胞指向化の増強を目指したナノ構造化 DNA の開発）

２０１９

LIAO Wenqing

Contents

Preface ..... **- 1 -**

Chapter 1 Development of G-quadruplex Structured CpG ODN for Enhanced Stability and Immunoreactivity ..... **- 3 -**

1.1 Introduction ..... - 4 -

1.2 Materials and Methods ..... - 5 -

1.3 Results ..... - 8 -

1.3.1 Formation of GQ structured CpG ODN ..... - 8 -

1.3.2 Effect of the sequence on GQ structured CpG ODN formation ..... - 10 -

1.3.3 Interference of dimeric GQ structure formation by adding thymine ..... - 11 -

1.3.4 Secretion of TNF-α of single-stranded CpG ODNs with G-tracts ..... - 11 -

1.3.5 Secretion of Cytokines induced by GQ structured CpG ODN ..... - 12 -

1.3.6 Uptake of GQ structured CpG ODN ..... - 14 -

1.3.7 Stability of GQ structured CpG ODN in serum ..... - 15 -

1.4 Discussion ..... - 16 -

Chapter 2 Development of Mannose-modified Nanostructured DNA for Targeted Delivery of CpG ODN to Antigen-presenting Cells ..... **- 19 -**

2.1 Introduction ..... - 20 -

2.2 Materials and Methods ..... - 21 -

2.3 Results ..... - 27 -

2.3.1 Synthesis of mannosylated ODN1668 ..... - 27 -

2.3.2 Preparation of CpG ODN-loaded hexapodna ..... - 27 -

2.3.3 Measurement of T_m ..... - 28 -

2.3.4 Surface expression of mannose receptors on cells ..... - 29 -

2.3.5 TNF-α release from mouse peritoneal macrophages and RAW264.7 cells ..... - 29 -

2.4 Discussion ..... - 31 -

Chapter 3 Development of Mannose-modified G-quadruplex Structured CpG ODN for Targeted Delivery to Antigen-presenting Cells ..... **- 33 -**

3.1 Introduction ..... - 34 -

3.2 Materials and Methods ..... - 34 -
3.3 Results ..... - 37 -
3.3.1 Low GQ structure formation after modification with the synthesized mannose motif ..... - 37 -
3.3.2 GQ structure formation after modification with a mannose motif with a shorter linker ..... - 39 -
3.3.3 Detection of surface MR expression in J774.1 cells ..... - 40 -
3.3.4 IL-6 release by J774.1 or RAW264.7 cells in response to treatment with mannose-modified CpG ODNs ..... - 40 -
3.3.5 TNF-α release from mouse peritoneal macrophages after treatment of mannose-modified CpG ODNs ..... - 41 -
3.4 Discussion ..... - 42 -
Conclusion ..... **- 44 -**
List of Publications ..... **- 46 -**
Other Publications ..... **- 47 -**
Acknowledgement ..... **- 48 -**
References ..... **- 49 -**

Preface

Nucleic acid medicine is expected as a next generation medicine because of its diverse targets and high specificity. The oligodeoxynucleotide containing unmethylated cytosine-phosphate-guanine, or CpG ODN, is derived from viruses and bacteria, and is a danger signal to stimulate innate immune cells[1]. There are mainly three types of CpG ODNs, A, B, and C types, having different immune activities. The receptor for CpG ODN is Toll-like receptor 9, which is an endosomal receptor in antigen presenting cells like dendric cells and macrophages. Therefore, the CpG ODN can stimulate and enhance the innate immunity so that it has been found as the therapeutic agonist against cancers, allergic or infectious diseases, and so on. For example, a licensed vaccine for B-type hepatitis uses CpG ODN as an adjuvant. Therefore, many drug delivery systems, or DDS, for CpG ODN have been developed[2].

Recent advances on DNA nanotechnology have greatly widened the potential applications for nucleic acid drug delivery. Therefore, many studies reported that delivery systems like liposomes, micelles, gold nanoparticles and DNA nanoparticles are crucial carriers to achieve efficient delivery of CpG ODN to target cells[3-5]. For example, Department of Biopharmaceutics and Drug Metabolism has developed the polypod-like structured nucleic acid, or polypodna, a DNA nanostructure constructed with 3 or more ODNs for efficient delivery of CpG ODNs to antigen presenting cells[6]. In particular, the relationship between the structure and the immunostimulatory activity has been studied. It suggested that the polypodna led to higher cellular uptake and immune activity compared with the conventional, single stranded CpG ODN.

However, two improvable points are deserved to be considered in practical application (Figure Pre.1). On the one hand, the ideal DNA nanocarrier for CpG ODN delivery should be constructed by only CpG sequences with necessary numbers of nucleotides, so that leads to a simple design with low

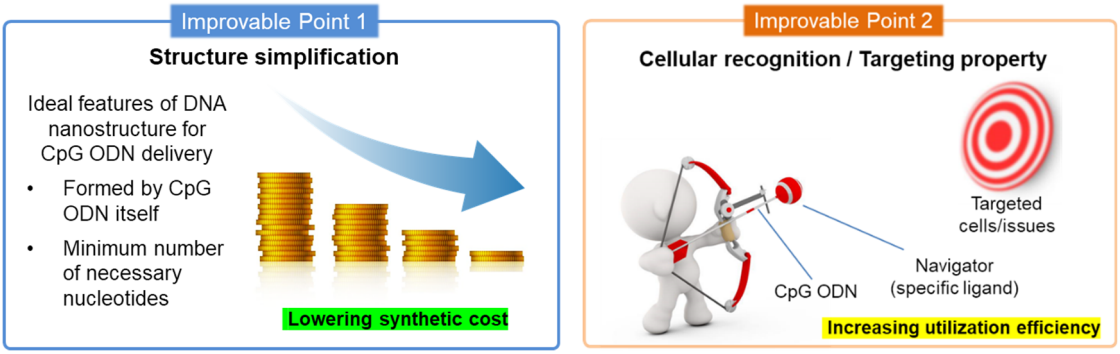

Figure Pre.1. Improvable points in practical application of CpG ODN.

synthetic cost. On the other hand, cellular uptake of DNA nanostructures by immune cells just relies on the concentration and stereochemical structures, therefore, endowing them cellular targeting property can increase their utilization efficiency.

In this thesis, I developed simple strategies to deliver the CpG ODN (Figure Pre.2) by nanostructuration using G-quadruplex just introducing several guanines into the sequence of CpG ODN to realize the structure simplification for delivery system of CpG ODN (Chapter 1), and to modify the DNA nanostructures including polypod-like structured nucleic acid (Chapter 2) and G-quadruplex structured CpG ODN (Chapter 3) by mannose to increase the delivery efficiency of CpG ODN to antigen-presenting cells.

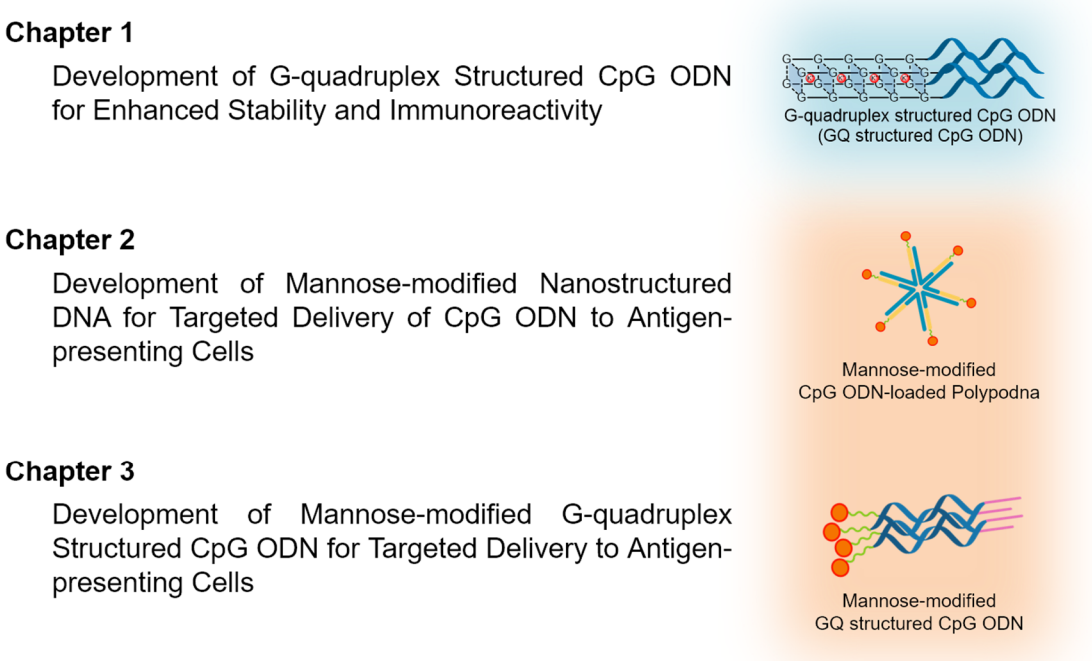

Figure Pre.2. Constitution of the thesis. The blue background is corresponding to improvable point 1, and the orange background is corresponding to improvable point 2.

Chapter 1

Development of G-quadruplex Structured CpG ODN for Enhanced Stability and Immunoreactivity

1.1 Introduction

G-quadruplex (GQ) structure, a stable helical secondary nucleic acid structure, is formed by stacking of G-quartets, a guanine tetrad tightened by Hoogsteen interaction with coordinating metal cations (e.g. Na^+, K^+)[7]. GQ structures exist naturally at the 3′-end of chromosomes, which is well known as telomeric region protecting chromosomes from degradation by nucleases. In addition, in some transcriptional regulatory regions of multiple genes and oncogenes, the formation of GQ structure adjusts specific gene expression and influence their biological activities[8, 9]. Taking the advantage of its unique structural property and stability, GQ structure has been widely studied as an important component part in nucleic acid nanotechnology including nanocarrier design for drug delivery[10]. For example, a GQ-based micelle has been constructed which could be disrupted to result in cargo by adding a complementary or a combination with aptamer which is responsible to ATP release[11]. Moreover, by introduction a poly-G-tract at the 5′-end of an cation peptide modified antisense oligonucleotide, not only the stability but also the cellular uptake were significantly enhanced, even the transfection process was in the absence of lipofectamine[12]. Nevertheless, only a few applications of GQ structures to nucleic acid delivery have been reported.

Nucleic acid drugs are expected as next generation drugs because of their diverse targets and high specificity. Unmethylated cytosine-phosphate-guanine ODN (CpG ODN) has been studied as one of the nucleic acid drugs that stimulate innate immunity. Mechanically, after internalization by antigen presenting cells (APCs) like macrophages and dendric cells, CpG ODN binds to Toll-like receptor 9 (TLR9) expressed in endosomes, and then triggers MyD88-dependent inflammatory responses[13]. As a licensed vaccine for B-type hepatitis, HEPLISAV-B® (HBsAg1018) developed by Dynavax Technologies Corporation (Berkeley, CA) utilizes phosphorothioate-stabilized CpG 1018 as a TLR9 agonist[2]. Enhancing stability and increasing utility (cellular uptake) are major issues for the application of nucleic acid drugs including CpG ODN. In particular, as the target of CpG ODN, APCs show highly size-dependent internalization behaviors[4]. Therefore, many studies have reported that delivery systems like liposomes, micelles, gold nanoparticles, and DNA nanoparticles are crucial carriers to achieve efficient delivery of CpG ODN to target cells[3-5].

Three classes of CpG ODNs, each of which has different immune activities, have been mainly studied so far[1]. Structurally, class A CpG ODN consists of a palindromic central CpG sequence with phosphodiester backbone and terminal phosphonothioate-backboned poly-G tracts. Class A CpG ODN forms a hairpin structure using the central sequence and, then forms aggregates through the G-tracts. This high-order structure of class A CpG ODN leads to high immunostimulatory activity compared with single-stranded class B CpG ODN[14]. Therefore, introducing G-tract into class B CpG ODN

might improve its both biological stability and immunostimulatory activity. Recently, Hoshi *et al.* reported that the stability in serum, immunostimulatory activity and cellular uptake of a phosphodiester class B CpG ODN were improved by addition of several G-tracts to the ODN[15]. This result provides a new approach for class B CpG ODN delivery, and the increased stability could avoid the use of phosphorothioate linkages which are associated with renal toxicity[16, 17]. Despite its potential usefulness in the delivery of CpG ODN, several G-tracts in one sequence required to design a long sequence, which is linked with an increased cost[18]. More importantly, it is quite difficult to obtain GQ-structured CpG ODN with precise structure[7]. Therefore, I considered whether the addition of only one G-tract is useful to obtain GQ-structured CpG ODN with precise structural properties, as well as increased biological stability and high immunostimulatory activity.

In this chapter, I focused on a phosphodiester-backboned CpG ODN (CpG1668) with the same sequence as CpG ODN 1668, a class B CpG ODN, and simply added 5 guanines (G-tract) to either 5′-, 3′-, or internally within the sequence, and investigated their structural properties and immunostimulatory activity. The results revealed that the introduction of only one G-tract to CpG1668 was sufficient to form parallel GQ structure and able to significantly increase the immunostimulatory activity. In addition, the effect of G-tract and its position upon immunostimulatory activity of CpG1668 was also discussed.

1.2 Materials and Methods

Preparation of GQ structured CpG ODN and CpG ODN loaded tetrapodna

Phosphodiester ODNs were purchased from Integrated DNA Technologies, Inc. (Coralville, IA, USA), and Alexa Fluor 488-labeled ODNs were purchased from Japan Bio Services Co., LTD.（Saitama, Japan). The sequences of the ODNs used are summarized in Table 1 and Table 2. GQ structured CpG ODN were prepared as follows. Each ODN (0.5 mM) in solution containing 150 mM KCl was annealed according to the protocol described by Mohri *et al*.[6]. CpG1668 loaded tetrapod-like structured DNA (tetrapodna) was prepared according to the protocol described by Takahashi *et* al.[19], and used as another nanostructured CpG ODN for comparison.

Polyacrylamide gel electrophoresis

The formation of GQ structured CpG ODN was confirmed by polyacrylamide gel electrophoresis (PAGE) (6% polyacrylamide gel) at 200 V, 4 ºC for 30 min. Each DNA sample (0.1 μg) was applied to the gel for PAGE. 20 bp DNA ladder was purchased from Takara (Tokyo, Japan). ODNs were

visualized by ethidium bromide (EtBr) (NIPPON GENE Co., Ltd., Tokyo, Japan) staining and observed using a LAS4000 imaging system (FUJIFILM, Tokyo, Japan).

Table 1. Sequences of CpG1668 and its derivatives. The name 1668(X′-G_5) means G_5 is at the X′-end. 1668(X′-4-G_5) means G_5 is at X′-end before/after 4 bases. 1668(X′-ΔY, Z′-G_5) means Y bases at X′-end are deleted from the sequence of CpG1668, and a G_5 is added at Z′-end of the sequence.

Name	Sequence (5′ to 3′)	Base number
CpG1668	TCC ATG ACG TTC CTG ATG CT	20
1668(5′-G_5)	**GGG GG**T CCA TGA CGT TCC TGA TGC T	25
1668(5′-4-G_5)	TCC A**GG GGG** TGA CGT TCC TGA TGC T	25
1668 (mid-G_5)	TCC ATG ACG TT**G GGG G**CC TGA TGC T	25
1668(3′-4-G_5)	TCC ATG ACG TTC CTG A**GG GGG** TGC T	25
1668(3′-G_5)	TCC ATG ACG TTC CTG ATG CT**G GGG G**	25
1668(5′-TG_5)	**T GGG GG**T CCA TGA CGT TCC TGA TGC T	26
1668(3′-G_5T)	TCC ATG ACG TTC CTG ATG CT**G GGG G T**	26
1668(3′-Δ3, 3′-G_5)	TCC ATG ACG TTC CTG AT**G GGG G**	22
1668(3′-Δ4, 3′-G_5)	TCC ATG ACG TTC CTG A**GG GGG**	21
1668(5′-G_5, 3′-Δ5)	**GGG GG**T CCA TGA CGT TCC TG	20
1668(3′-Δ5, 3′-G_5)	TCC ATG ACG TTC CTG **GGG GG**	20
1668(5′-G_5, 3′-Δ7)	**GGG GG**T CCA TGA CGT TCC	18
1668(3′-Δ7, 3′-G_5)	TCC ATG ACG TTC C**GG GGG**	18
1668(5′-G_5, 5′-Δ2, 3′-Δ5)	**GGG GG**T CTG ACG TTC CTG	18
1668(5′-Δ2, 3′-Δ5, 3′-G_5)	TCT GAC GTT CCT G**GG GGG**	18
1668(5′-G_5) GpC	**GGG GG**T CCA TGA GCT TCC TGA TGC T	25
1668(3′-G_5) GpC	TCC ATG AGC TTC CTG ATG CT**G GGG G**	25
1668(5′-G_5, 3′-Δ5) GpC	**GGG GG**T CCA TGA GCT TCC TG	20
5′-Alexa Fluor 488-CpG1668	Alexa 488-TCC ATG ACG TTC CTG ATG CT	20
CpG1668-Alexa Fluor 488-3′	TCC ATG ACG TTC CTG ATG CT-Alexa 488	20
1668(5′-G_5)-Alexa Fluor 488-3′	**GGG GG**T CCA TGA CGT TCC TGA TGC T-Alexa 488	25
5′-Alexa Fluor 488-1668(3′-G_5)	Alexa 488-TCC ATG ACG TTC CTG ATG CT**G GGG G**	25

Table 2. Sequences of Tetrapodna. The underlined bases are the parts hybridize with CpG1668.

Name	Sequence (5′ to 3′)	Base number
Tetra-1	TAGCA GCACA TCAGG TTCTG AGCCT TGCTG CAAGC ATCAG GAACT TCATG GA	52
Tetra-2	TGCAG CAAGG CTCAG ATCTG CTCAA GCCTG CAAGC ATCAG GAACT TCATG GA	52
Tetra-3	TGCAG GCTTG AGCAG ACAGA GCCTT GAGCC TAAGC ATCAG GAACT TCATG GA	52
Tetra-4	TAGGC TCAAG GCTCT GACCT GATGT GCTGC TAAGC ATCAG GAACT TCATG GA	52

Circular dichroism spectroscopy

CpG ODNs were diluted in 150 mM KCl or distilled H_2O to a concentration of 5 μM. Circular dichroism (CD) spectra were measured with a circular dichroism spectrometer (J-820/805, JASCO Co., Nihon Bunko, Tokyo, Japan) at 37 °C using a quartz cell of 1 mm optical path length (JASCO Co., Nihon Bunko, Tokyo, Japan). All samples were scanned from 200 ~ 320 nm in a rate of 100 nm/min, a band width of 2 nm. The results were integrated from 10 scans.

Cell culture

Mouse macrophage-like RAW264.7 cells were cultured in RPMI 1640 (Nissui Pharmaceutical Co., Ltd., Japan) supplemented with 10% heat-inactivated fetal bovine serum (Gibco, Thermo Fisher Scientific Inc., Waltham, MA, USA), penicillin G (100 U/mL), streptomycin (100 μg/mL) and L-glutamine (2 mmol/L) (FUJIFILM Wako Pure Chemical Co., Japan) in a humidified incubator containing 5% CO_2 at 37 °C.

TNF-α and IL-6 release from RAW264.7 cells

RAW264.7 cells were seeded into a 96-well plate at a density of 5×10^4 cells/well and incubated for 24 h before treatment. Then, DNA samples diluted by Opti-modified Eagle's medium (Opti-MEM, Thermo Fisher Scientific Inc., Waltham, MA, USA) were added to RAW264.7 cells at the CpG ODN concentration of 100 nM after aspiration of supernatant, and the cells were further incubated for 8 h at 37 °C. Then, the supernatant was collected and the concentrations of tumor necrosis factor (TNF)-α and interleukin (IL)-6 were determined by enzyme-linked immunosorbent assay (ELISA) following the manufacturer's protocol (TNF-α: BioLegend, Inc., San Diego, CA, USA; IL-6: Thermo Fisher

Scientific Inc., Waltham, MA, USA).

Uptake of GQ structured CpG ODN by RAW264.7 cells

Alexa Fluor 488-labaled CpG ODNs were prepared as above and used for cellular uptake experiments. RAW264.7 cells were seeded into 96-well plates at a density of 1×10^5 cells/well and incubated for 24 h before treatment. RAW264.7 cells were incubated with 100 nM Alexa Fluor 488-labeled ODN diluted with Opti-MEM for 2 h at 37 °C. Cells were then washed twice with PBS and harvested. Then, mean fluorescence intensity (MFI) of the cells was determined using a flow cytometer (Gal lios Flow Cytometer; Beckman Coulter, Miami, FL, USA). Data were analyzed using FlowJo software (version 8.8.4; Beckman Coulter).

Stability of GQ structured CpG ODN in serum

GQ structured CpG ODN (0.5 mM, 1 μL, 3.8 μg) prepared as above was added into FBS (9 μL), then incubated in a humidified incubator at 37 ºC. Then, 250 mM ethylenediaminetetraacetic acid disodium (1 μL) was added into the mixture to stop the reaction. The amounts of remaining ODN were detected by PAGE. All samples were applied to the gel for PAGE after the same fold dilution in volume. The CpG ODNs were visualized by EtBr staining and observed using a LAS4000 imaging system (Fujifilm, Tokyo, Japan).

1.3 Results

1.3.1 Formation of GQ structured CpG ODN

Considering the length of CpG1668, as an initial attempt, 5 guanines were simply added to the 5′-end of CpG1668 to obtain [1668(5′-G_5)]. To confirm whether 1668(5′-G_5) formed GQ structure, CpG ODNs in solution containing different concentrations of KCl were annealed, then applied to PAGE analysis (Figure 1A). 1668(5′-G_5) annealed in distilled H_2O gave the band of single-stranded ODN. CD spectra (Figure 1B) showed that 1668(5′-G_5) annealed in distilled H_2O and CpG1668 had a negative peak around 240-250 nm and a positive peak around 280 nm, which are typical spectral features for single-stranded, random coil DNA. In contrast, two sharp peaks, negative peak at 240 nm and positive peak at 260 nm, were detected when 1668(5′-G_5) was annealed in solution containing 150 mM KCl, which are specific spectral featured for parallel GQ structure[20, 21]. These results suggested that the addition of only one G-tract was sufficient for the formation of parallel GQ structure.

Because the concentration of potassium is quite lower than 150 mM in physiological environment,

the stability of GQ structure formed in 150 mM NaCl was conducted (Figure 2). As a comparison, the ODN annealed in 150 mM NaCl was used for test of GQ structure formation with sodium. Before application to gel of PAGE, all samples were diluted to a solution in 150 mM NaCl. As a result, although GQ structure formed in 150 mM NaCl, the conversion efficiency from single-stranded ODNs to GQ structured ODNs was quite lower than in 150 mM KCl. In addition, the GQ structure was also detected in 150 mM NaCl diluent (390 μM KCl after dilution). These results suggested that potassium was better than sodium in GQ structure formation, and GQ structure was stable in 150 mM NaCl once it was constructed in KCl.

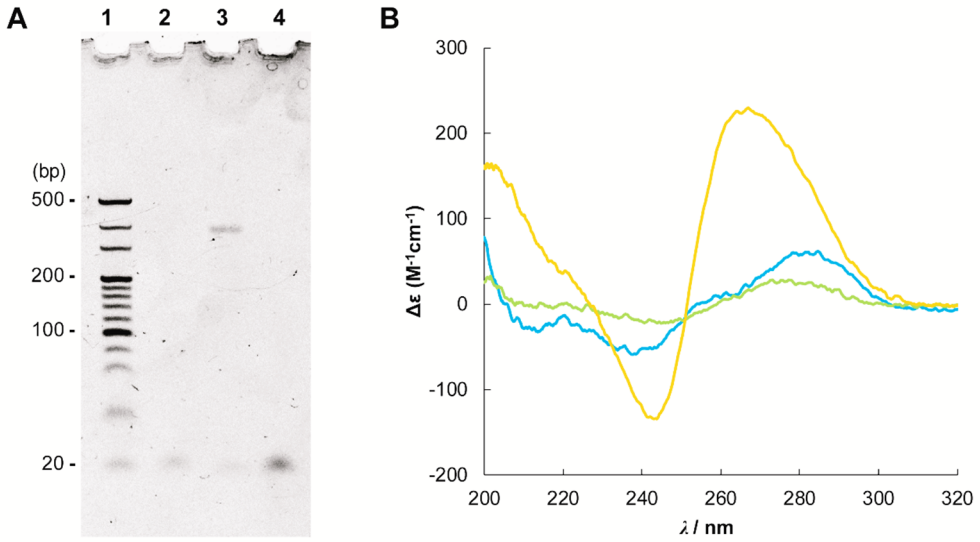

Figure 1. Confirmation of GQ structure formation. (**A**) PAGE analysis of CpG ODNs. Lane 1, 20 bp ladder; lane 2, CpG1668; lane 3, 1668(5′-G_5); lane 4, 1668(5′-G_5) annealed in distilled H_2O. (**B**) Circular dichroism spectra of CpG1668 and 1668(5′-G_5)s. Green line, CpG1668; blue line, 1668(5′-G_5) annealed in distilled H_2O; yellow line, 1668(5′-G_5) annealed in 150 mM KCl.

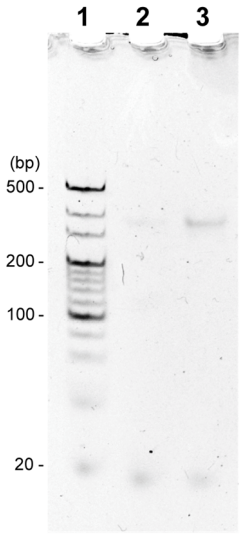

Figure 2. GQ structure formation in 150 mM and stability of GQ structure in 150 mM NaCl. PAGE analysis of CpG ODNs. All samples were diluted to a solution with 150 mM NaCl before PAGE. Lane 1, 20 bp ladder; lane 2, 1668(5′-G_5) annealed in 150 mM NaCl; lane 3, 1668(5′-G_5) annealed in 150 mM KCl.

1.3.2 Effect of the sequence on GQ structured CpG ODN formation

The effect of the position of G-tract on the GQ structure formation was evaluated (Figure 3). I designed several ODNs by shifting the G-tract in 1668(5′-G_5) away from 5′-end to 3′-end. All ODNs were annealed in 150 mM KCl and CD spectra showed all these sequences formed parallel GQ structures (Figure 3A, lane 2-4; Figure 3B, upper panel). In PAGE analysis, the band of the GQ structures decreased once the G-tract was shifted far from 5′-end [1668(5′-G_5)] and their sizes read by ladder were about half of 1668(5′-G_5). Then, the effect of ODN length on the formation of GQ structure was examined using PAGE (Figure 3A, lane 5-7). A conversion efficiency from single-stranded ODNs to GQ structure ODNs could be improved by shortening 5 bases from 3′-end for

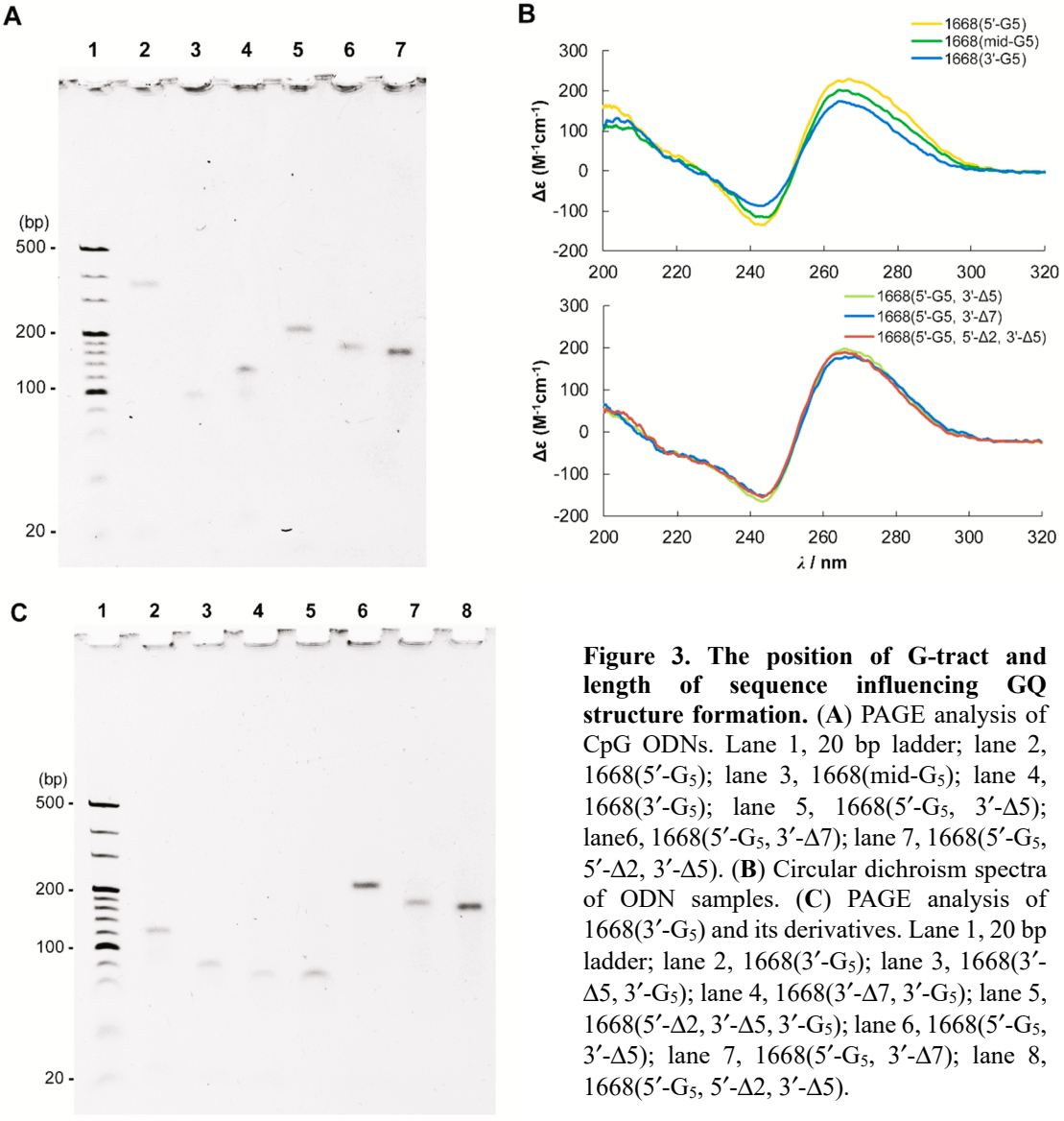

Figure 3. The position of G-tract and length of sequence influencing GQ structure formation. (**A**) PAGE analysis of CpG ODNs. Lane 1, 20 bp ladder; lane 2, 1668(5′-G_5); lane 3, 1668(mid-G_5); lane 4, 1668(3′-G_5); lane 5, 1668(5′-G_5, 3′-Δ5); lane6, 1668(5′-G_5, 3′-Δ7); lane 7, 1668(5′-G_5, 5′-Δ2, 3′-Δ5). (**B**) Circular dichroism spectra of ODN samples. (**C**) PAGE analysis of 1668(3′-G_5) and its derivatives. Lane 1, 20 bp ladder; lane 2, 1668(3′-G_5); lane 3, 1668(3′-Δ5, 3′-G_5); lane 4, 1668(3′-Δ7, 3′-G_5); lane 5, 1668(5′-Δ2, 3′-Δ5, 3′-G_5); lane 6, 1668(5′-G_5, 3′-Δ5); lane 7, 1668(5′-G_5, 3′-Δ7); lane 8, 1668(5′-G_5, 5′-Δ2, 3′-Δ5).

1668(5′-G_5). A similar tendency was observed with 1668(3′-G_5). These results suggested that the shorter the sequence, the better the conversion. In addition, all these ODNs were also formed parallel GQ structures (Figure 3B, lower panel). Interestingly, in all cases, the sizes of 3′-end GQ structures were about half of 5′-end GQ structures (Figure 3C).

1.3.3 Interference of dimeric GQ structure formation by adding thymine

Previous works indicated that the additional thymine at 5′- or 3′-end interfered the formation of high-order structures and stabilized the GQ structure[22, 23]. Then, one thymine was added to the 5′-end of 1668(5′-G_5) or the 3′-end of 1668(3′-G_5) (Figure 4). The additional T on the 3′-end of 1668(3′-G_5) hardly changed the band position of 1668(3′-G_5). On the other hand, a half-sized structure, which the position of band was the same as 1668(3′-G_5), was detected from [1668(5′-TG_5)]. These results not only support the formation of GQ structure dimer from 1668(5′-G_5), but also the additional T could interfere the formation of dimeric GQ structure.

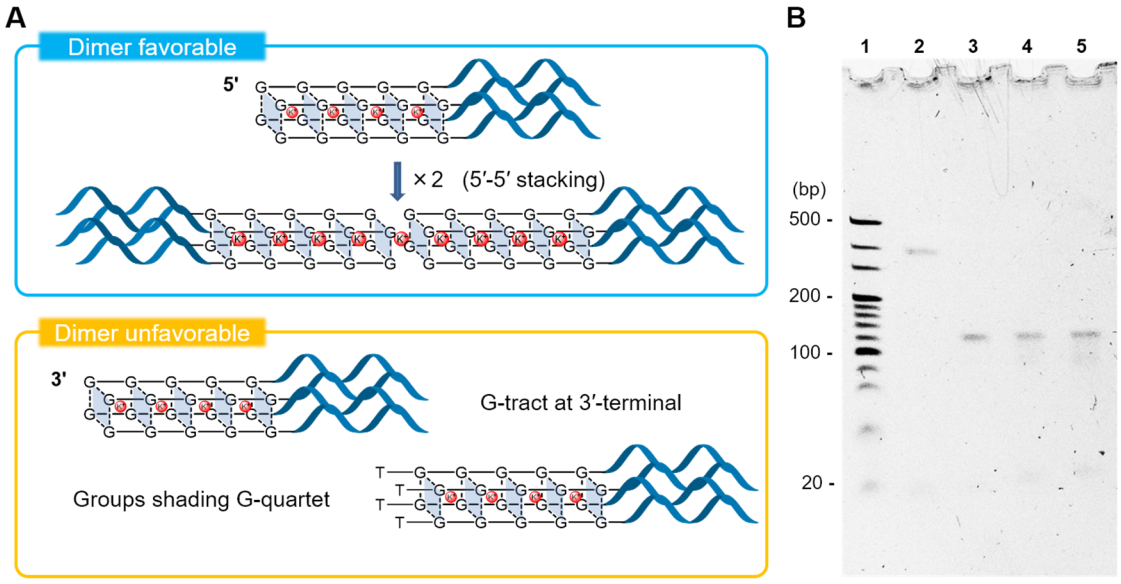

Figure 4. Effect of additional T on GQ structure formation. (**A**) Structural features affecting favorable and unfavorable dimeric structure formation. (**B**) PAGE analysis of CpG ODNs with or without T adjacent to the G-tract, annealed in 150 mM KCl. Lane 1, 20 bp ladder; lane 2, 1668(5′-G_5); lane 3, 1668(5′-TG_5); lane 4, 1668(3′-G_5); lane 5, 1668(3′-G_5T).

1.3.4 Secretion of TNF-α of single-stranded CpG ODNs with G-tracts

Initially, I evaluated whether the addition of G-tract would influence the immunostimulatory activity of CpG1668 in its single-stranded form. All ODNs were annealed in distilled H_2O to obtain single-stranded ODNs and added to RAW264.7 cells at an identical concentration of CpG ODN (1 μM). After incubation for 8 h, the release of TNF-α was examined by ELISA (Figure 5A). 1668(5′-

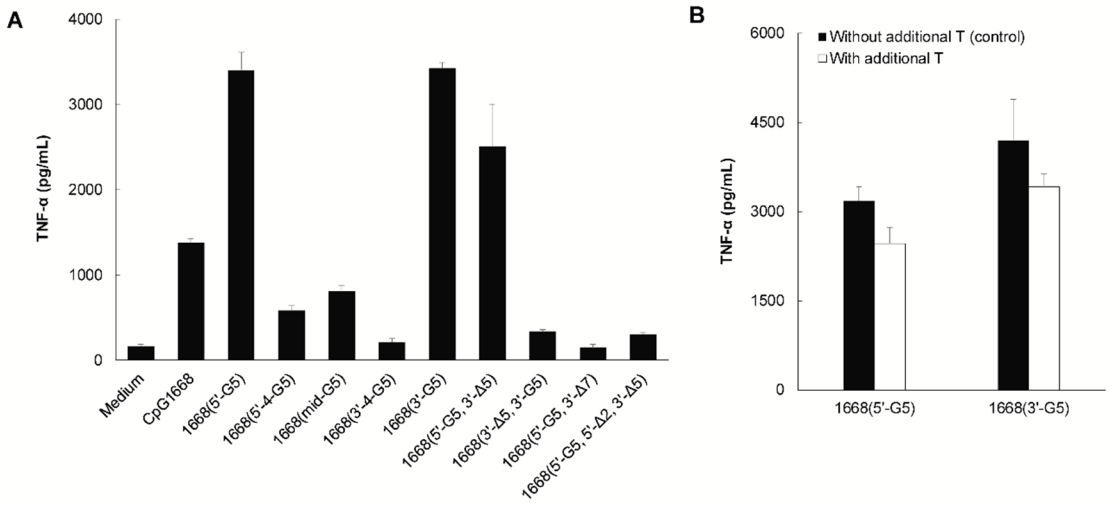

Figure 5. Effect upon immunostimulatory activity after addition of G-tracts into sequences. CpG1668 and other sequences in single-stranded status were added to RAW264.7 cells at a final concentration of 1 μM. The concentration of released TNF-α was measured. The filled bars (■) represent the sequence with an additional T in front of/behind G-tract of the control sequence represented in hollow bars (□). Results are expressed as the mean ± S.D. (n = 4).

G_5) and 1668(3′-G_5) induced higher TNF-α secretion by RAW264.7 cells as two-fold as CpG1668. However, 1668(5′-4-G_5), 1668 (mid-G_5) and 1668(3′-4-G_5), whose G-tract was closer to CG sequence, induced low TNF-α release compared with CpG1668. The activity almost hardly changed by removing 5 bases from 3′-end of 1668(5′-G_5), namely 1668(5′-G_5, 3′-Δ5). On the other hand, further shortening the sequence dramatically decreased the release of TNF-α [1668(5′-G_5, 3′-Δ7) and 1668(5′-G_5, 5′-Δ2, 3′-Δ5)]. In contrast to 1668(5′-G_5), the TNF-α release also dramatically decreased when the G-tract was shifted from 5′-end to 3′-end in case of 1668(5′-G_5, 3′-Δ5). In addition, additional T [1668(5′-TG_5) and 1668(3′-G_5T)] hardly affected the secretion of TNF-α from RAW264.7 cells (Figure 5B).

1.3.5 Secretion of Cytokines induced by GQ structured CpG ODN

Next, all ODNs were prepared in GQ structure and the immunostimulatory activity was evaluated by adding 100 nM ODN samples to RAW264.7 cells (Figure 6). 1668(5′-G_5), 1668(3′-4-G_5), 1668(3′-G_5), 1668(5′-G_5, 3′-Δ5) and 1668(5′-G_5, 3′-Δ7) induced higher TNF-α (Figure 6A, B) and IL-6 (Figure 6C) release compared with the single-stranded CpG ODN. However, no improvement was found with 1668(5′-4-G_5), 1668(mid-G_5) and 1668(5′-G_5, 5′-Δ2, 3′-Δ5). It is worth mentioning that 1668(3′-G_5) was more effective than CpG1668-loaded tetrapod-like nucleic acid (tetrapodna) (CpG1668/tetrapodna), which was previously developed in Department of Biopharmaceutics and Drug Metabolism[6, 19]. Furthermore, additional T to 1668(5′-G_5) reduced the TNF-α release, whereas additional T to 1668(3′-G_5) hardly changed the release (Figure 6B).

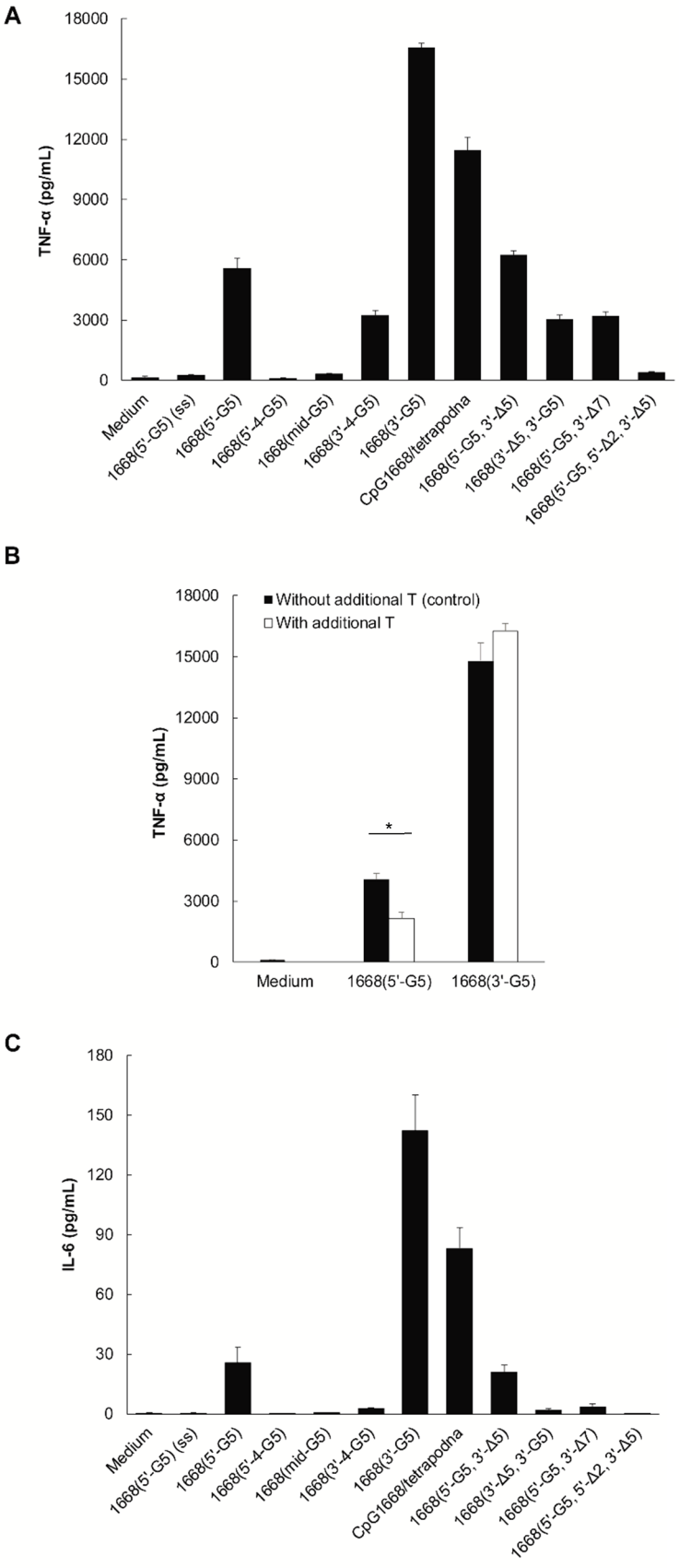

Figure 6. Enhanced immune activity by introduction of GQ structure.

1668(5′-G_5)(ss), other GQ structured CpG ODNs and CpG1668/Tetrapodna were added to RAW264.7 cells at a final concentration of 100 nM. The concentration of released (**A**, **B**) TNF-α and (**C**) IL-6 were measured. The filled bars (■) represent the sequence with an additional T in front of/behind G-tract of the control sequence represented in hollow bars (□). Results are expressed as the mean ± S.D. (n = 4). *$p < 0.05$, two-tailed unpaired Student's *t*-test.

Interestingly, 1668(3′-Δ5, 3′-G_5) induced lower TNF-α release than 1668(5′-G_5, 3′-Δ5). This was an opposite tendency to 1668(5′-G_5) and 1668(3′-G_5). Therefore, I briefly investigated how the distance of G-tract from the CG motif influence the immunostimulatory activity (Figure 7A). A dramatic decrease of TNF-α release occurred when 4 bases were deleted [1668(3′-Δ4, 3′-G_5)] although 3 base deletion only slightly weakened the activity [1668(3′-Δ3, 3′-G_5)].

To understand whether GQ structure also induces secretion of TNF-α, the ODNs bearing GC sequences were evaluated, since TLR9 activation is abolished by the rearrangement of the CG sequence to GC[24]. As a result, no TNF-α secretion was detected (Figure 7B). This result suggested that CG sequence but not GQ structure activates TLR9.

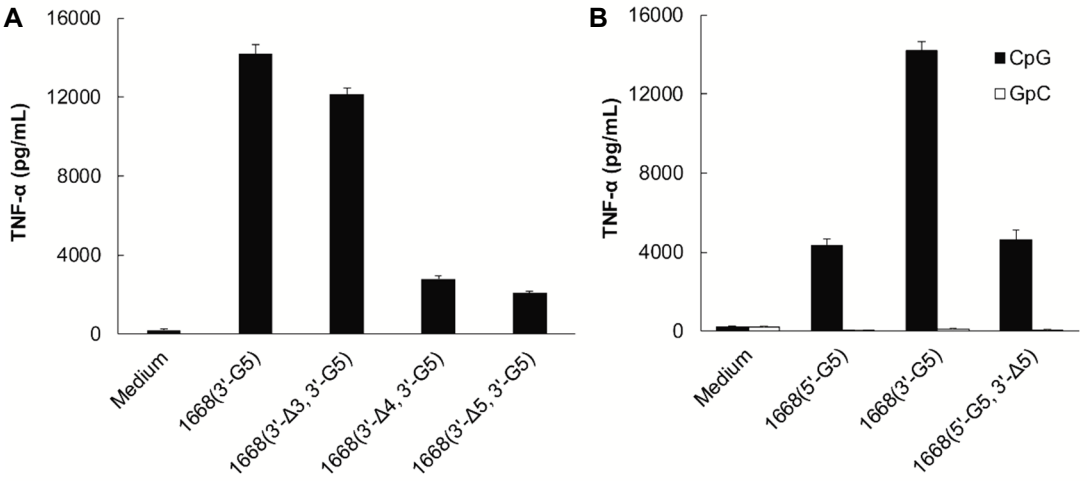

Figure 7. Distance of G-tract to CG sequence influencing immunostimulatory activity and CG sequence but not GQ structure activating TLR9. GQ structured CpG ODNs were added to RAW264.7 cells at a final concentration of 100 nM. The concentration of released TNF-α were measured. (**A**) TNF-α release from RAW264.7 cells by GQ structured CpG ODNs with different distance of G-tract to CG sequence. (**B**) TNF-α release from RAW264.7 cells by GQ structured CpG ODNs with or without CG sequence. The filled bars (■) represent the ODN with CpG sequence but GpC sequence in hollow bars (□). Results are expressed as the mean ± S.D. (n = 4).

1.3.6 Uptake of GQ structured CpG ODN

To understand the relationship between the cellular uptake and immunostimulatory activity, the uptake of ODNs labeled with Alexa Fluor 488 by RAW264.7 cells was examined (Figure 8). The MFI of cells added with GQ structured CpG ODN was significantly higher than that of cells added with single-stranded ODNs. 1668(5′-G_5) gave around 2-fold higher MFI than 1668(3′-G_5). Taking it into consideration that 1668(5′-G_5) and 1668(3′-G_5) mainly formed dimeric and monomeric GQ structures respectively (Figure 3A), it can be said that the cellular uptake efficiency was comparable between

these two structures. This result also suggested higher internalization of GQ structured CpG ODN can be achieved by dimer formation.

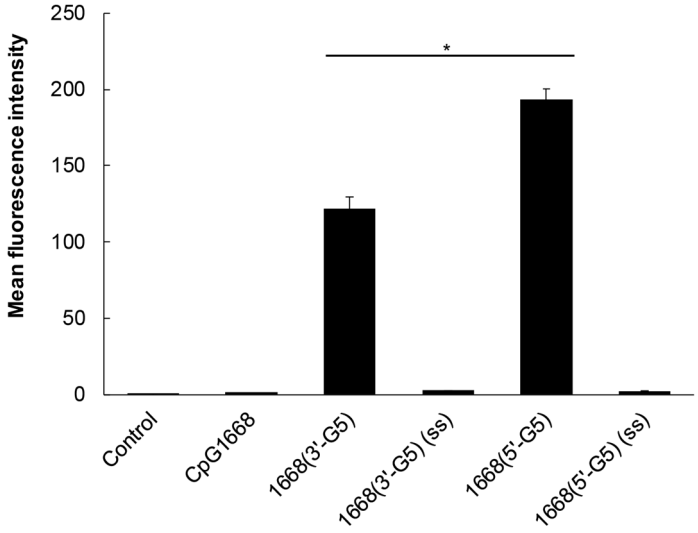

Figure 8. Uptake of GQ structured CpG ODNs by RAW264.7 cells. RAW264.7 cells were incubated with 100 nM Alexa Fluor 488-labeled GQ structured CpG ODNs for 2 h at 37 °C. Mean fluorescence intensity (MFI) of the cells was determined using a flow cytometer. Results are expressed as the mean ± S.D. (n = 4). *$p < 0.05$, two-tailed unpaired Student's *t*-test.

1.3.7 Stability of GQ structured CpG ODN in serum

As for the reason why 1668(5′-G_5) and 1668(3′-G_5) induced different secretion of TNF-α and IL-6 even though they had similar uptake efficiency, I considered whether the stability of GQ structured CpG ODN was related to the immunostimulatory activity. A previous work showed CpG ODN with several G-tracts in sequence, which was able to form GQ structure, had enhanced stability in serum[15]. However, the different effect of G-tracts on 5′-end or 3′-end was not studied. Therefore, 1668(5′-G_5) and 1668(3′-G_5) were representatively selected for stability confirmation. All CpG ODNs were added to FBS and their degradation was analyzed by PAGE (Figure 9A). The size and intensity of 1668(5′-G_5) decreased along with time, whereas the size of 1668(3′-G_5) hardly changed although decrease in intensity was detected.

Moreover, to rule out the influence of dimer formation, stability of 1668(5′-TG_5) and 1668(3′-G_5T) was tested, which both only formed a monomer (Figure 9B). The size of 1668(3′-G_5T) hardly changed with time after incubation in FBS, but 1668(5′-TG_5) was apparently decomposed in as short as 1 h.

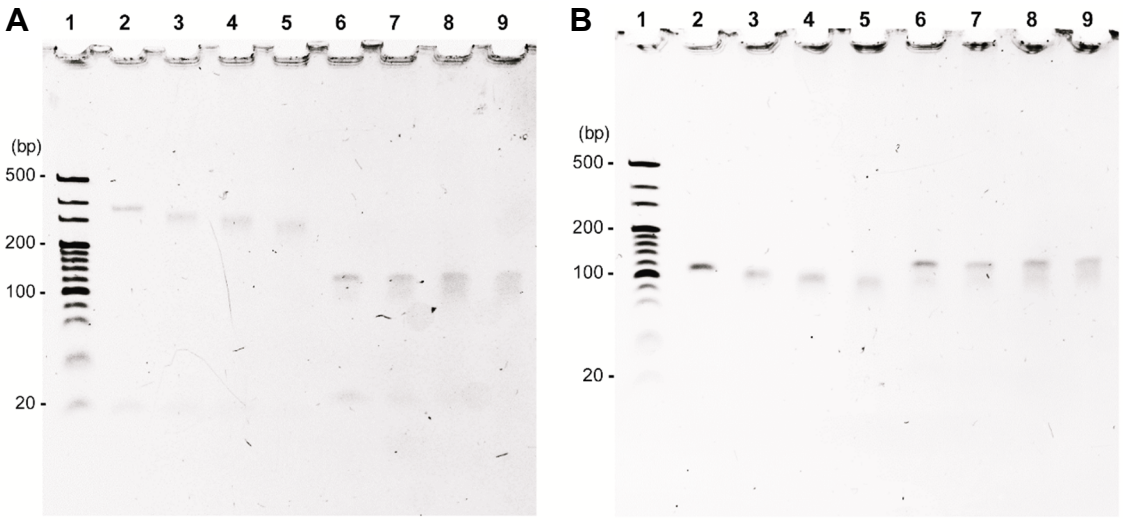

Figure 9. Stability of GQ structure in serum. PAGE analysis of (**A**) 1668(5′-G_5) (lane 2-5) and 1668(3′-G_5) (lane 6-9), (**B**) 1668(5′-TG_5) (lane 2-5) and 1668(3′-G_5T) (lane 6-9) after addition into FBS and the stability in serum was confirmed in a time scale. Lane 1, 20 bp ladder; lane 2 and 6, 0 h; lane 3 and 7, 1 h; lane 4 and 8, 2 h; lane 5 and 9, 4 h.

1.4 Discussion

Stability and delivery to target cells are the main issues upon the application of CpG ODN as adjuvants. These issues can be solved by nanostructuration because nanostructured DNAs were more resistant to DNase degradation, and more efficiently taken up by cells via endocytosis than single-stranded DNAs[4, 14]. Therefore, as one of natural stable structure, GQ triggered my interest for its application and further investigation to delivery of CpG ODNs. A parallel GQ structure which consisted of 4 identical DNA molecules with G-tracts[7, 22] attracted me, because its potential to form nanostructure may increase the cellular uptake of CpG ODN. Single-stranded DNA with one poly-G tract can form parallel GQ structure in the buffer with proper cations, especially potassium[15, 22]. In addition, at least 4 guanines are necessary for stable GQ structure formation. In this study, a phosphodiester-backboned CpG ODN (CpG1668), which has the same sequence of class B CpG ODN 1668, was selected as a CpG ODN for GQ structuration. By simply adding 5 guanines at the 5′-end of CpG1668, it successfully afforded the GQ structured CpG ODN by G-quadruplex formation (Figure 1). In addition, GQ structured CpG ODN brings high loading efficiency of CpG ODN compared with other DNA nanocarriers developed so far since it was formed only with CpG ODNs.

The position of G-tracts in sequence influences the conformation of GQ structure. G-tract at the 5′-end [1668(5′-G_5)] led to the formation of a bigger structure than at 3′-end [1668(3′-G_5)] or in the middle [1668(mid-G_5)] (Figure 3A). Besides, CD spectra showed that a typical positive peak at around 260 nm and a negative peak at around 240 nm were detected when all ODNs with G-tracts were

annealed in 150 mM KCl (Figure 3B). These results indicated parallel GQ structures formed in all these ODNs. In addition, adding a T in front of the G-tract limited the 1668(5′-G_5) to form an about 2-fold higher structure and lead to form a structure with the same size as 1668(3′-G_5), but no effect in case of 1668(3′-G_5) (Figure 4). A previous work revealed GQ structures at 5′-end were thermodynamically favorable to form dimer by 5′-5′ stacking but unfavorable in the case of 5′-3′ or 3′-3′ stacking pattern [25]. Therefore, these results suggested that 1668(5′-G_5) formed dimeric GQ structures, but other ODNs formed monomeric ones.

Unlike very short sequences like TG_4T[22, 26], single-stranded ODN was detectable in 1668(5′-G_5) and 1668(3′-G_5) after the formation of GQ structures. Shortening the length of sequence improved the conversion from single-stranded ODNs to GQs (Figure 3A). I speculated that the repulsion between the negative charges of the sequences adjacent to the G-tract interfered the formation of GQ structure. Therefore, the free single-stranded part of the sequence might disturb the strong Hoogsteen interaction among four ODNs. In addition, the results also indicated that the sequences of 25 bases or shorter with 5 guanines would give better GQ structure formation efficiency.

Not only the structure of TLR9 and its interaction with CpG ODN, but also relationship between CpG ODN sequence and its immunostimulatory activity have been extensively studied[24, 27, 28]. CpG ODN should contain at least 20 bases but not longer than 29 bases for efficient activation of TLR9. Therefore, the sequence shorter than 20 [e.g. 1668(5′-G_5, 3′-Δ7) and 1668(5′-G_5, 5′-Δ2, 3′-Δ5)] did not apparently induce TNF-α release (Figure 5A). In addition, the proper interaction of CpG ODN with TLR9 is important upon immune activation, especially the second cytosine from the 5′-end was reported to be crucial for CpG ODN coordinating to TLR9[24, 27]. This could explain that 1668(5′-G_5, 3′-Δ7) but not 1668(5′-G_5, 5′-Δ2, 3′-Δ5) induced TNF-α release after GQ structure formation. It is worth mentioning that G-tract increased the immunostimulatory activity of CpG1668 no matter which terminal was tagged. This result replenished the relationship between CpG ODN sequence and its immunostimulatory activity.

The formation of GQ structure significantly increased the immunostimulatory activity (Figure 6), cellular uptake efficiency (Figure 8) and stability (Figure 9) of CpG ODN. Previous works indicated that the existence of poly guanines at the 3′-end of phosphodiester CpG ODNs significantly enhanced cellular uptake and TNF-α production, but the TNF-α production was diminished when guanines were placed at 5′-end[29, 30]. Although the authors confirmed the GQ structure formation in their investigations, GQ structured CpG ODNs were not prepared under definite and specified conditions. In addition, they did not properly investigate the relationship between structure and the immunostimulatory activity. In this study, G-tract at 3′-end gave around 2-fold TNF-α release

compared with at 5′-end but cellular uptake of similar amount of CpG ODNs was detected (Figure 6A). As for the modification position of fluorescence probes in cellular uptake study, 3′-end for 1668(5′-G_5) and 5′-end for 1668(3′-G_5) were modified. The purpose of changing the modification position was to avoid the modifier disturbing dimer formation in 1668(5′-G_5) and GQ structure formation. To rule out the influence from different modification position, the cellular uptake of CpG1668 modified with 5′- and 3′-Alexa Fluor 488 was tested, and no difference was detected (data not shown). The difference of cytokine secretion between 1668(5′-G_5) and 1668(3′-G_5) might be attributed to two reasons. Firstly, placing G-tracts at 3′-end leaves the second cytosine and CpG motif free so that makes it easier to interact with TLR9, however, when G-tract located at 5′-end, the bulk and stable G-quadruplex structure limited its interaction with TLR9. Secondly, the stability investigation indicated the nuclease in serum was prone to decompose DNA from 3′-end and the 3′-end GQ structure showed a superior ability to protect CpG ODN. Importantly, the 3′-end GQ structured CpG ODN was more stable so that remained more immunologically active CpG ODNs to activate TLR9. Previous work suggested DNA including CpG ODN is prone to be cleaved from the 3′-end by exonuclease[31]. Therefore, GQ structure at 3′-end can significantly increase resistance to nuclease so that keep the existence of more valid active CpG ODN (Figure 9). In addition, ODN containing poly guanines have been reported to show an increase in cellular uptake efficiency since poly guanines binds with scavenger receptors on the cell surface[29, 32]. Therefore, the scavenger receptor-mediated endocytosis might also contribute to the improved cellular uptake of CpG ODN by GQ structure formation.

Chapter 2

Development of Mannose-modified Nanostructured DNA for Targeted Delivery of CpG ODN to Antigen-presenting Cells

2.1 Introduction

DNA containing the unmethylated cytosine-phosphate-guanine (CpG) motif, which is typically found in bacteria and viruses, is a danger signal to stimulate innate immune cells[33, 34]. Toll-like receptor 9 (TLR9), an endosomal receptor for CpG DNA, is expressed in antigen-presenting cells (APCs) like macrophages and dendric cells[34, 35]. Ligation of TLR9 triggers innate immune responses that can be useful for various diseases including cancers[36-38]. Synthetic oligodeoxynucleotides (ODNs) containing the CpG motif can mimic the immunostimulatory effects of bacterial and viral DNA. There are mainly three types of CpG ODNs having different immune activities[33], and their clinical application as immune adjuvants has been explored. For example, HEPLISAV-B®, which utilizes phosphorothioate-stabilized CpG 1018 as an adjuvant, is a licensed vaccine for treatment of B-type hepatitis[2, 39].

The direct administration of single-stranded CpG ODN should be economical and convenient because CpG ODN coordinates with TLR9 in the single-stranded form[27, 40, 41]. However, the vulnerability to some enzymes like DNase and low cellular uptake efficiency call for suitable carriers for the delivery of CpG ODNs to APCs[14]. Recent advances on DNA nanotechnology have provided various delivery systems for nucleic acid therapeutics, such as siRNA, miRNA, aptamer and, of course, CpG ODN[42]. Polypod-like structured nucleic acid, or polypodna, is a DNA nanostructure constructed with 3 or more ODNs that has been used for the efficient delivery of CpG ODNs to APCs[6, 43-47]. Compared with the conventional, single stranded CpG ODN, CpG ODN loaded on polypodna led to higher cellular uptake and immunostimulatory activity.

Previous study in Department of Biopharmaceutics and Drug Metabolism demonstrated that macrophage scavenger receptor 1 (MSR1), one of the scavenger receptors, was involved in the efficient uptake of polypodna depending on its structural complexity[48]. Further increase in the cell specificity and targeting efficiency of nanostructured DNAs to immune cells could be achieved by the use of receptor-ligand recognition[49]. This can be achieved by selecting a combination of a receptor that is expressed on target immune cells and a high-affinity ligand that selectively binds to the receptor. Among various receptors, C-type lectin receptors (CLRs), which often bind to glycan structures in a Ca^{2+}-dependent manner[50], are attractive targets because they are mainly expressed on APCs[51]. As a member of the CLRs, mannose receptor (MR), which can specifically recognize saccharides like mannose, is mostly expressed on the surface of macrophages and dendritic cells[52]. In addition, MR-mediated endocytosis has been studied and applied to achieve cell-specific delivery of bioactive compounds[53-55]. Recently, a mannosylated CpG ODN (Man-CpG ODN) has been developed, which showed both enhanced immunostimulatory activity and cellular internalization efficiency[56].

Therefore, I considered that combining Man-CpG ODN with polypodna could extensively increase the immunostimulatory activity of CpG ODNs.

In 2017, a hexapodna (the polypodna with 6 pods) backbone designed to be a versatile carrier for CpG ODNs has been developed[19]. Taking the advantage of this backbone, in this study, I first selected a phosphodiester CpG ODN with the same sequence as CpG ODN 1668, named it as ODN1668, and synthesized mannosylated ODN1668 (Man-ODN1668). Then, I developed a hexapodna loaded with Man-ODN1668, Man-ODN1668/hexapodna, and examined its usefulness to induce cytokine release from mouse peritoneal macrophages.

2.2 Materials and Methods

General

All synthetic operations were conducted with a standard Schlenk technique under argon atmosphere. Flash column liquid chromatography was performed using Kanto Chemical silica gel 60NO (spherical, 40–50 μm) (Kanto Chemical Co., Inc., Tokyo, Japan). Analytical thin layer chromatography (TLC) was performed on Merck Kieselge1 60 F254 (0.25 mm) plates (Merck KGaA, Darmstadt, Germany). Visualization was accomplished with 3% H_2SO_4 solution in methanol followed by heating.

Chemicals

Unless otherwise noted, commercially available chemicals were used as received. Pyridine (dehydrated), dichloromethane (super dehydrated), acetonitrile (super dehydrated), *N*-hydroxysuccinimide (NHS) were purchased from Fujifilm Wako Pure Chemical Industries, Ltd. (Osaka, Japan). D-(+)-Mannose, 5-hexen-1-ol, tin(IV) chloride (ca. 1 mol/L in dichloromethane), 1-(3-dimethylaminopropyl)-3-ethylcarbodiimide hydrochloride (EDC·HCl) were purchased from Tokyo Chemical Industry Co., Ltd. (Tokyo, Japan). Acetic anhydride, sodium periodate and Celite® 535RVZ were purchased from Nacalai Tesque, Inc. (Kyoto, Japan). All the other chemicals were of the highest grade available and were used without further purification.

Oligonucleotides

Phosphodiester ODNs were purchased from Integrated DNA Technologies, Inc. (Coralville, IA, USA). The oligonucleotide sequences were designed based on a previous work[19] (Table 3). ODN1668 has the same sequence as phosphorothioate CpG ODN 1668, and 5'-NH_2-ODN1668 was used for

mannosylated ODN1668 (Man-ODN1668) synthesis. The complementary sequence to the CpG motif (GACGTT) in hexa-1 to -6 was designed to have a single base mismatch (AACTTC) not to include CG sequence and to avoid TLR9 stimulation by these ODNs.

Table 3. Sequences of ODNs. All ODNs were phosphodiester backbone. /5AmMC6/, 5′ amino modifier C6.

Name	Sequence (5′ to 3′)	Base number
Hexa-1	TAGCA GCACA TCAGG TTCTG AGCCT TGCTG CAAGC ATCAG GAACT TCATG GA	52
Hexa-2	TGCAG CAAGG CTCAG ATCTG CTCAA GCCTG CAAGC ATCAG GAACT TCATG GA	52
Hexa-3	TGCAG GCTTG AGCAG ACAGA GCCTT GAGCC TAAGC ATCAG GAACT TCATG GA	52
Hexa-4	TAGGC TCAAG GCTCT GGAGG CTCTT AAGCT GCAGC ATCAG GAACT TCATG GA	52
Hexa-5	GCAGC TTAAG AGCCT CAGAG CTTGG CATAG CAAGC ATCAG GAACT TCATG GA	52
Hexa-6	TGCTA TGCCA AGCTC TACCT GATGT GCTGC TAAGC ATCAG GAACT TCATG GA	52
ODN1668	TCCAT GACGT TCCTG ATGCT	20
5′-NH_2-ODN1668	/5AmMC6/TCCAT GACGT TCCTG ATGCT	20

Apparatus

Proton and carbon nuclear magnetic resonance spectra (^{1}H NMR and ^{13}C NMR) were recorded on a JEOL JNM-ECZ400 (^{1}H at 399.78 MHz and ^{13}C at 100.53 MHz) spectrometer (JEOL Ltd., Tokyo, Japan) with solvent resonance as the internal standard (^{1}H NMR, $CHCl_3$ at 7.26 ppm; ^{13}C NMR, $CDCl_3$ at 77.0 ppm). ^{1}H NMR data are reported as follows: chemical shift multiplicity (s = singlet, d = doublet, t = triplet, q = quartet, m = multiplet), coupling constants (Hz), and integration.

Synthesis of 5-hexenyl 2,3,4,6-tetra-*O*-acetyl α-D-mannopyranoside (3)

D-Mannose pentaacetate (**2**) was synthesized according to previous report[57]. Briefly, to a solution of D-(+)-mannose (10 mmol, 1.80 g) in pyridine (20 mL), add acetic anhydride (63.4 mmol, 6.47 mg, 6.0 mL, 6.34 eq.) dropwise at room temperature (rt). The reaction mixture was further stirred at rt for 10 h. The resulting mixture was quenched by methanol and concentrated with toluene *in vacuo*

to yield a light-yellow oil (>99%). The crude residue was directly used for glycosylation of 5-hexen-1-ol. To a solution of compound **2** (0.53 mmol, 209.9 mg) in CH_2Cl_2 (7 mL), add $SnCl_4$ (1.0 mol/L in CH_2Cl_2, 0.5 mL, 1.0 eq.) dropwise. Then, 5-hexen-1-ol (0.58 mmol, 58.4 mg, 70.0 μL, 1.1 eq.) was immediately added into the reaction mixture with vigorous stir. The reaction mixture was further stirred at rt for 5 h. The resulting mixture was quenched by sat. $NaHCO_3$ (aq.) then poured into a separatory funnel and extracted by CH_2Cl_2 for three times. Organic layer was filtered through Celite® and concentrated. The crude residue was further purified on silica gel column (hexane : ethyl acetate = 3 : 1) to yield the desired product in a colorless oil liquid (62.5 mg, 27%).

^{1}H NMR (400 MHz, $CDCl_3$): δ = 5.79-5.69 (m, 1H), 5.28 (dd, J = 10.0, 3.4 Hz, 1H), 5.22 (d, J = 9.9 Hz, 1H), 5.18-5.16 (m, 1H), 4.98-4.88 (m, 2H), 4.74 (d, J = 1.7 Hz, 1H), 4.21 (dd, J = 12.2, 5.3 Hz, 1H), 4.04 (dd, J = 12.2, 2.4 Hz, 1H), 3.99-3.84 (m, 1H), 3.63 (dt, J = 12.1, 4.8 Hz, 1H), 3.40 (dt, J = 11.8, 4.8 Hz, 1H), 2.09 (s, 3H), 2.05-1.99 (m, 8H), 1.93 (s, 3H), 1.60-1.53 (m, 2H), 1.44-1.38 (m, 2H). **^{13}C NMR** (101 MHz, $CDCl_3$): δ = 170.42, 169.87, 169.69, 169.56, 138.20, 114.67, 97.38, 69.52, 68.96, 68.26, 68.11, 66.07, 62.35, 33.19, 28.49, 25.16, 20.71, 20.54, 20.51, 20.50 ppm. **MS** (ESI^+): Calcd. for $C_{20}H_{30}O_{10}Na^+$ $[M+Na]^+$: 453.1731. Found: m/z 453.1733.

Synthesis of 5-[(tetra-*O*-acetyl α-D-mannopyranosyl)oxyl] pentanoic acid (4)

To a solution of compound **3** (0.15 mmol, 62.5 mg) in CH_2Cl_2/CH_3CN (1:1, 0.64 mL), add $RuCl_3 \cdot H_2O$ (aq.) (1.29 mg/mL, 0.48 mL; 3 μmol, 0.62 mg, 2.1 mol %). Then, $NaIO_4$ (0.6 mmol, 127.9 mg, 4.15 eq.) was immediately added into the reaction mixture with vigorous stir. After 2 h, an additional $NaIO_4$ (0.6 mmol, 127.9 mg, 4.15 eq.) was added and the reaction mixture was further stirred at rt for 2 h. The resulting mixture was diluted by H_2O then poured into a separatory funnel and extracted by CH_2Cl_2 for three times. Organic layer was dried over $MgSO_4$ and concentrated *in vacuo* to yield a dark oil liquid. The crude residue was directly used for next reaction (53.5 mg, 82%, crude yield).

^{1}H NMR (400 MHz, $CDCl_3$): δ = 5.33 (dd, J = 10.0, 3.4 Hz, 1H), 5.28 (d, J = 9.8 Hz, 1H), 5.24-5.22 (m, 1H), 4.80 (d, J = 1.5 Hz, 1H), 4.27 (dd, J = 12.2, 5.4 Hz, 1H), 4.10 (dd, J = 12.2, 2.4 Hz, 1H), 3.99-3.95 (m, 1H), 3.71 (dt, J = 11.1, 5.0 Hz, 1H), 3.47 (dt, J = 11.0, 5.0 Hz, 1H), 2.42-2.39 (m, 2H), 2.15 (s, 3H), 2.10 (s, 3H), 2.04 (s, 3H), 1.99 (s, 3H), 1.75-1.67 (m, 4H). **^{13}C NMR** (101 MHz, $CDCl_3$): δ = 178.33, 170.70, 170.12, 169.98, 169.77, 97.57, 69.62, 69.11, 68.47, 67.89, 66.17, 62.52, 33.37, 28.53, 21.31, 20.89, 20.72, 20.69 ppm. **MS** (ESI^+): Calcd. for $C_{19}H_{28}O_{12}Na^+$ $[M+Na]^+$: 471.1473. Found: m/z 471.1473.

Synthesis of 2,5-dioxopyrrolidin-1-yl 5-[(tetra-*O*-acetyl α-D-mannopyranosyl)oxyl] pentanate

(5)

To a solution of compound **4** (0.119 mmol, 53.5 mg) and *N*-hydroxysuccinimide (0.125 mmol, 14.4 mg, 1.05 eq.) in CH_2Cl_2 (1 mL) was added 1-(3-dimethylaminopropyl)-3-ethylcarbodiimide hydrochloride (0.125 mmol, 24.0 mg, 1.05 eq.). The reaction mixture was stirred at rt for 6 h. The resulting mixture was quenched by H_2O then poured into a separatory funnel and extracted by CH_2Cl_2 for three times. Organic layer was washed by brine and dried over Na_2SO_4, then concentrated in vacuo. The crude residue was directly used for modification of CpG1668 (65.4 mg, >99%, crude yield, dark oil liquid).

^{1}H NMR (400 MHz, $CDCl_3$): δ = 5.29 (dd, J = 10.0, 3.4 Hz, 1H), 5.24 (d, J = 9.8 Hz, 1H), 5.21-5.19 (m, 1H), 4.78 (d, J = 1.5 Hz, 1H), 4.24 (dd, J = 12.2, 5.3 Hz, 1H), 4.06 (dd, J = 12.2, 2.2 Hz, 1H), 3.96-3.92 (m, 1H), 3.71 (dt, J = 11.3, 4.9 Hz, 1H), 3.47 (dt, J = 11.2, 4.9 Hz, 1H), 2.80 (s, 4H), 2.64 (t, J = 7.0 Hz, 2H), 2.12 (s, 3H), 2.06 (s, 3H), 2.01 (s, 3H), 1.95 (s, 3H), 1.86-1.78 (m, 2H), 1.75-1.69 (m, 2H) ppm. **^{13}C NMR** (101 MHz, $CDCl_3$): δ = 170.56, 169.95, 169.75, 169.66, 169.08, 168.23, 97.48, 69.49, 68.97, 68.40, 67.47, 66.10, 62.42, 30.47, 28.11, 25.50, 21.33, 20.80, 20.65, 20.61, 20.59 ppm. **MS** (ESI^+): Calcd. for $C_{23}H_{31}NO_{14}Na^+$ $[M+Na]^+$: 568.1637. Found: m/z 568.1645.

Synthesis of mannosylated ODN1668 (Man-ODN1668)

To a mixture solution of Na_2CO_3-$NaHCO_3$ buffer (0.33 M, pH = 9, 60 μL) and DMSO (64 μL), add 5′-NH_2-ODN1668 (20 nmol, 1 mM in distilled H_2O, 20 μL). Then compound **5** (20 μL, 0.5 M in DMSO, 40 μL) was added into the mixture above. After conducting a light vortex and centrifuge, the mixture was kept at rt over night for further reaction. The reactant was purified via a Zeba spin desalting column (7K MWCO, Thermo Fisher Scientific Inc., USA) according to manufacturer's protocol followed by lyophilization to yield a white powder. The product was resolved in distilled H_2O. The formation of Man-ODN1668 was confirmed by matrix assisted laser desorption ionization-time of flight mass spectrometry (MALDI-TOF MS, JMS-S3000, JEOL Ltd., Japan). **MS** Calcd.: 6501.4. Found: 6501.1. The yield was 93%, confirmed by Nanodrop 2000/2000c (Thermo Fisher Scientific Inc., USA).

Preparation of polypodna

All ODNs involved in polypodna formation were mixed in appropriate molar ratios, heated to 95 °C, and then gently cooled to 4 ° C. Details of the preparation protocol were described in a previous manuscript[6].

Polyacrylamide gel electrophoresis

The formation of hexapodnas was confirmed by polyacrylamide gel electrophoresis (PAGE) (6% polyacrylamide gel) at 200 V for 30 min at rt. Each DNA sample was applied into the gel for PAGE in 50 ng. 100 bp DNA ladder was purchased from Takara (Tokyo, Japan). ODNs were visualized by staining with ethidium bromide (EtBr; Nippon Gene Co., Ltd., Tokyo, Japan) staining and observed using a LAS4000 imaging system (Fujifilm, Tokyo, Japan).

Measurement of melting temperature

Hexapodnas were diluted in 150 mM NaCl to 250 μg/mL. Melting temperature (T_m) was measured with a spectrophotometer (JASCO J-730, JASCO, Tokyo, Japan) using a quartz cell of 1 mm optical path length (JASCO). All samples were scanned from 20 °C to 95 °C in a rate of 1 °C/min and the absorbances were recorded per 0.5 °C.

Animals

C57BL/6N mice (female, 6-week-old) were purchased from Sankyo Labo Service Co., Inc. (Tokyo, Japan). All animal experiments are with the approval of the Animal Research Committee of the Faculty of Pharmaceutical Sciences, Tokyo University of Science.

Isolation of mouse peritoneal macrophages

Elicited macrophages were harvested from the peritoneal cavity of C57BL/6N mice 3 days after intraperitoneal injection of 2 mL 2.9% thioglycolate medium (Nissui Pharmaceutical Co. Ltd., Tokyo, Japan). Cells were washed, then suspended in RPMI 1640 (Nissui Pharmaceutical Co., Ltd., Japan) supplemented with 10% heat-inactivated fetal bovine serum (Gibco, Thermo Fisher Scientific Inc., Waltham, MA, USA), penicillin G (100 U/mL), streptomycin (100 μg/mL) and L-glutamine (2 mmol/L) (Fujifilm Wako Pure Chemical Industries, Ltd., Japan) in a humidified incubator containing 5% CO_2 at 37 °C. The cells were plated on 10 cm dish. After incubation for 2 h, nonadherent macrophages were washed off with culture medium, then attached cells were regarded as peritoneal macrophages and harvested for further experiments.

Culture of mouse macrophage-like RAW264.7 cells

Mouse macrophage-like RAW264.7 cells were cultured in RPMI 1640 (Nissui Pharmaceutical Co., Ltd., Japan) supplemented with 10% heat-inactivated fetal bovine serum (Gibco, Thermo Fisher Scientific Inc., Waltham, MA, USA), penicillin G (100 U/mL), streptomycin (100 μg/mL) and L-

glutamine (2 mmol/L) (FUJIFILM Wako Pure Chemical Co., Japan) in a humidified incubator containing 5% CO_2 at 37 °C.

Identification for expression of surface mannose receptor on cells

The direct immunofluorescence staining of surface mannose receptor of mouse peritoneal macrophages and RAW264.7 cells were conducted following the manufacturer's protocol (Rat anti mouse CD206:Alexa Fluor® 488, Bio-Rad Laboratories Inc., CA, USA). Briefly, 1×10^6 cells were washed and suspended in 90 μL cold (4 ºC) PBS/BSA buffer, then add 10 μL anti-CD206 antibody into the cells, mix well and incubate at 4 ºC in dark. After 1 h incubation, cells were centrifuged and washed by PBS/BSA. After centrifuge, cells were resuspended in 200 μL cold PBS and determined using a flow cytometer (Gal lios Flow Cytometer; Beckman Coulter, Miami, FL, USA). Data were analyzed using FlowJo software (version 8.8.4; Beckman Coulter).

TNF-α release from peritoneal macrophages

Mouse peritoneal macrophages were seeded into a 96-well plate at a density of 1×10^5 cells/well and incubated for 24 h before treatment. Then, DNA samples diluted with Opti-modified Eagle's medium (Opti-MEM, Gibco, Thermo Fisher Scientific) were added to cells at the ODN1668 concentration of 2.4 μM after aspiration of supernatant, and the cells were further incubated for 8 h at 5% CO_2, 37 °C. Then, the supernatant was collected and the concentrations of tumor necrosis factor (TNF)-α were determined by enzyme-linked immunosorbent assay (ELISA) following the manufacturer's protocol (BioLegend, Inc., San Diego, CA, USA).

TNF-α release from RAW264.7 cells

Mouse peritoneal macrophages were seeded into a 96-well plate at a density of 5×10^4 cells/well and incubated for 24 h before treatment. Then, DNA samples diluted with Opti-modified Eagle's medium (Opti-MEM, Gibco, Thermo Fisher Scientific) were added to cells at the ODN1668 concentration of 1.2 μM after aspiration of supernatant, and the cells were further incubated for 8 h at 5% CO_2, 37 °C. Then, the supernatant was collected and the concentrations of tumor necrosis factor (TNF)-α were determined by enzyme-linked immunosorbent assay (ELISA) following the manufacturer's protocol (BioLegend, Inc., San Diego, CA, USA).

2.3 Results

2.3.1 Synthesis of mannosylated ODN1668

The synthesis consists of two parts: (1) the synthesis of the mannose motif and (2) the coupling (Figure 10). The 5-hexen-1-ol was glycosylated with mannose pentaacetate to give compound **3**. Then, the oxidation of **3** converted the double bond to a carboxylic group. The compound **4** reacted with *N*-hydroxysuccinimide to give the mannose motif **5**. Finally, by mixing 5′-NH_2-ODN1668 and **5** in buffer followed by hydrolysis, Man-ODN1668 was successfully synthesized with a yield of 93%, which was identified by MALDI-TOF mass spectrometry.

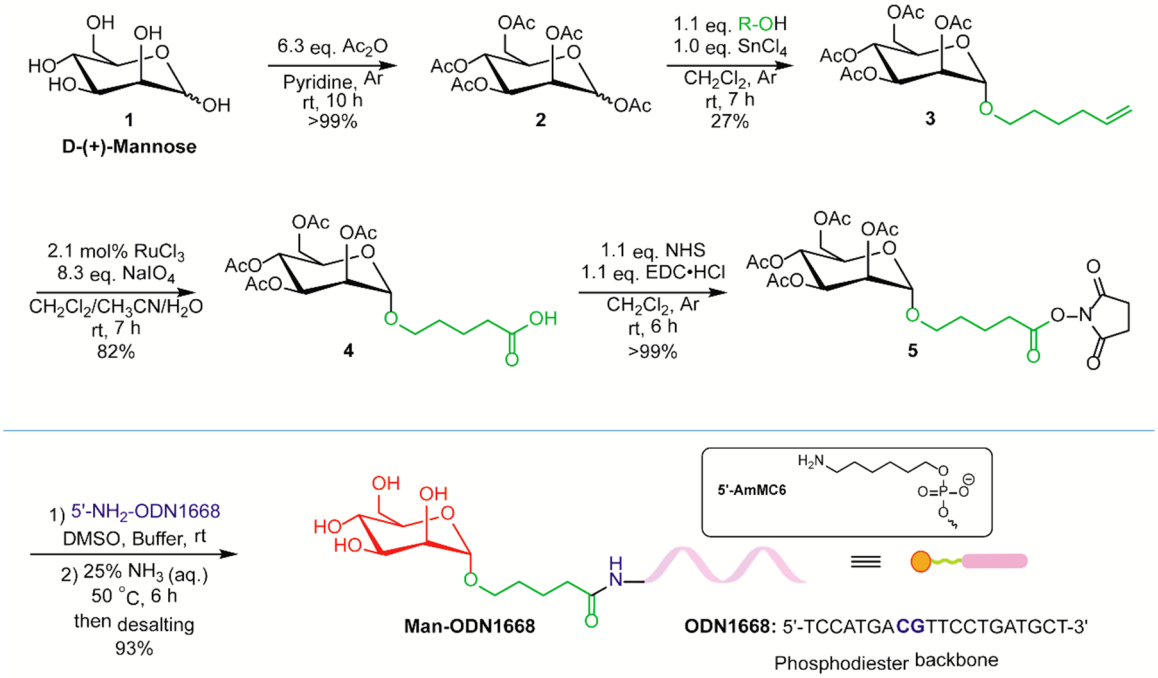

Figure 10. Synthesis of mannose modified ODN1668.

2.3.2 Preparation of CpG ODN-loaded hexapodna

A hexapodna backbone containing no CG sequences was constructed as previously reported[19]. For construction, ODN1668 or Man-ODN1668 was mixed with six ODNs that forms the hexapodna in a stoichiometric ratio of 6:1 to obtain six ODN1668 (Man-ODN1668)-loaded hexapodna. Two protocols were tested to confirm the construction of ODN1668-loaded hexapodna (Figure 11A). In the first protocol, all the ODNs were annealed in one step. Another one was to prepare the hexapodna backbone first, then added ODN1668 or Man-ODN1668 to the preformed hexapodna. The polyacrylamide gel electrophoresis results (Figure 11B) showed that all the DNA samples had a single

band, indicating that both protocols were efficient for the formation. The bands of the hexapodna backbone were shifted upward by the addition of ODN1668, and the mannose modification made the band shifted upward a little bit further. This result suggested the success of Man-ODN1668-loaded hexapodna (Man-ODN1668/hexapodna). In this work, the ODN1668/hexapodna and Man-ODN1668/hexapodna were constructed by annealing the mixture of all ODNs in one step.

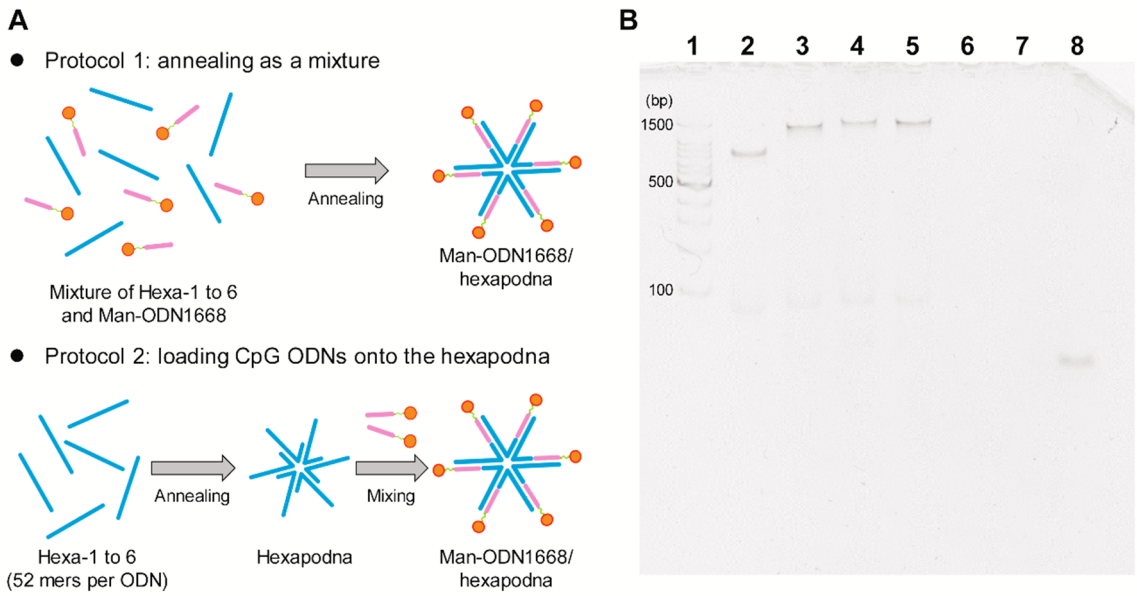

Figure 11. Construction and confirmation of ODN1668 loaded hexapodna. (**A**) Two protocols for construction of ODN1668 loaded hexapodna. (**B**) The formation of hexapodnas was confirmed by electrophoresis, which was run on a 6% polyacrylamide gel at 200 V for 30 min at room temperature. Lane 1, 100 bp ladder; lane 2, hexapodna; lane 3, ODN1668/hexapodna; lane 4, Man-ODN1668/hexapodna (protocol 1); lane 5, Man-ODN1668/hexapodna (protocol 2); lane 6, ODN1668; lane 7, Man-ODN1668; lane 8, Hexa-6.

2.3.3 Measurement of T_m

To check whether the thermal stability of ODN1668/hexapodna was changed by the mannose modification of ODN1668, the T_m was measured (Table 4). The T_m values of hexapodna, ODN1668/hexapodna, and Man-ODN1668/hexapodna were comparable. This indicated that the loading of ODN and the mannose modification hardly influenced the thermal stability of hexapodna.

Table 4. T_m values of DNA samples.

Structure	T_m (°C)
Hexapodna	59.3
ODN1668/hexapodna	57.5
Man-ODN1668/hexapodna	57.5

2.3.4 Surface expression of mannose receptors on cells

To discriminate whether the mannose modification works for specific binding, prior to the evaluation of immunostimulatory activity, the surface mannose expression of cells was identified. After being marked by Alexa Fluor 488 labeled anti-CD206 antibody, mouse peritoneal macrophages or RAW264.7 cells were collected and applied to flow cytometry (Figure 12). As the result, almost all peritoneal macrophages expressed surface mannose receptor but not in case of RAW264.7 cells.

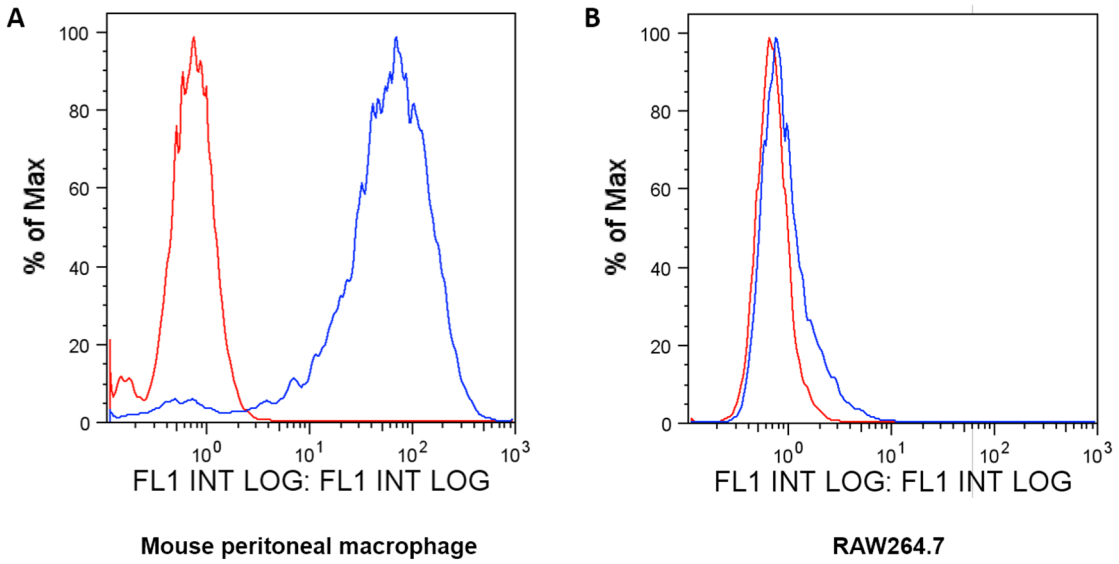

Figure 12. Surface expression of mannose receptor. Mouse peritoneal macrophages (**A**) and RAW264.7 cells (**B**) were labelled by Alexa Fluor 488-antiCD206 antibody. The red line represents cells without labelling (control) and blue line represents cells labelled (stained) by Alexa Fluor 488-anti CD206 antibody. Cells were collected and analyzed by flow cytometry and 1×10^4 cells were counted for analysis.

2.3.5 TNF-α release from mouse peritoneal macrophages and RAW264.7 cells

ODN1668, Man-ODN1668, hexapodna, ODN1668/hexapodna and Man-ODN1668/hexapodna were added to mouse peritoneal macrophage at the same amount of ODN1668 (0.24 nmol). Figure 13 shows the release of TNF-α from the cells at 8 h after addition of the samples. The mannose modification only slightly affected the TNF-α release by ODN1668. No significant TNF-α release was observed when hexapodna backbone was added. Compared with single-stranded CpG ODNs, a higher TNF-α release was observed by ODN1668- or Man-ODN1668-loaded hexapodna. Man-ODN1668/hexapodna induced two times higher TNF-α release than ODN1668/hexapodna. However, no difference was detected in RAW264.7 cells (Figure 14). These results indicated that the combination of mannose modification and incorporation into hexapodna is an effective approach for enhancing the immunostimulatory activity of CpG ODN, especially to MR positive immune cells.

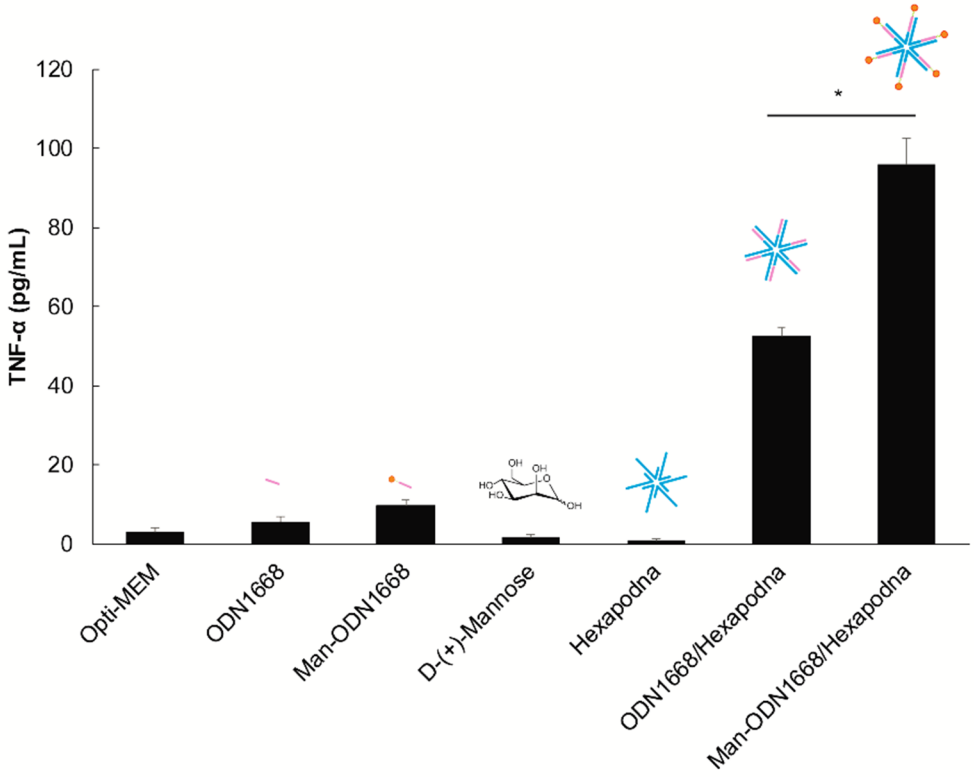

Figure 13. Enhanced TNF-α release of CpG ODN loaded hexapodna by mannose modification. All DNA samples diluted in Opti-MEM were added to mouse peritoneal macrophages at a final concentration of 2.4 μM in ODN1668. After incubation for 8 h, the cell media (supernatant) was collected and the concentration of TNF-α was measured. Results are expressed as the mean ± S.D. of four independent samples. **p* < 0.05, two-tailed unpaired Student's *t*-test.

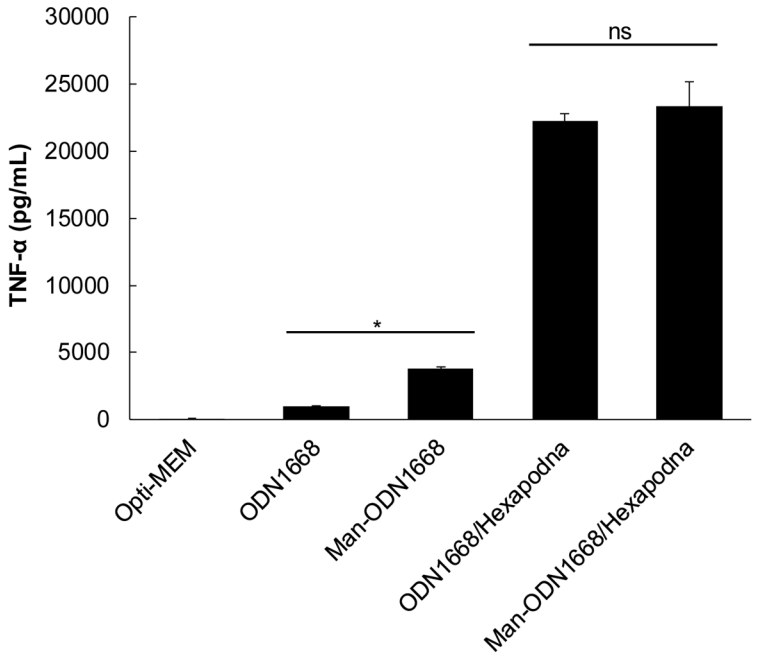

Figure 14. No enhanced TNF-α release detected from RAW264.7 cells. All DNA samples diluted in Opti-MEM were added to mouse macrophage like RAW264.7 cells at a final concentration of 1.2 μM in ODN1668. After incubation for 8 h, the cell media (supernatant) was collected and the concentration of TNF-α was measured. Results are expressed as the mean ± S.D. of four independent samples. **p* < 0.05, two-tailed unpaired Student's *t*-test. ns, not significant.

2.4 Discussion

One of the important issues for nucleic acid therapeutics is an efficient delivery to targeted sites. The polypodna previously developed in Department of Biopharmaceutics and Drug Metabolism has been proven available for the efficient delivery of CpG ODN to APCs[6]. In particular, the tripodna and hexapodna containing no CpG sequences have been shown to be a suitable carrier for CpG ODN delivery[19]. Considering that some problems like stability and targeting efficiency might exist for its *in vivo* application, I developed Man-ODN1668 and succeeded in one-pot synthesis of Man-ODN1668/hexapodna (Figure 10).

Mouse peritoneal macrophages were used because the cells express both TLR9 and macrophage mannose receptor (Figure 12A)[58, 59]. Mannose modification at the 5′-terminal of ODN will endow it not only with the affinity to mannose receptors, but also with improved biological stability. A slightly higher TNF-α release by single-stranded Man-ODN1668 than single-stranded ODN1668 could be explained by the following two possible reasons. First, the affinity of mannosylated ligands to the macrophage mannose receptor is highly dependent on the multivalency of mannose[60]. Because Man-CpG ODN has only one mannose unit per molecule, its affinity to the receptor could be low. Second, the 5′-terminal modification of ODN with mannose would slightly improve the biological stability of ODN by blocking the access of DNase to the ODN. Compared with ODN1668/hexapodna, Man-ODN1668/hexapodna was effective in inducing TNF-α release. This improvement could be explained by the structural properties of Man-ODN1668/hexapodna, in which six Man-ODN1668s were incorporated into one hexapodna backbone. This design could increase the density of mannose units, which then might lead to efficient recognition by the mannose receptor.

Man-ODN1668 induced higher TNF-α release than ODN1668 from RAW264.7 cells which hardly expressed surface mannose receptors. As mentioned above, these results could be explained as follows. 5′-terminal modification slightly improved the biological stability of ODN against DNase and the hydrophobic alkyl linker in the mannose motif might increase the interaction of Man-ODN1668 with cell membrane so that the modified CpG ODN had higher possibility to be taken up by cells. However, no difference in induced TNF-α release was detected from RAW264.7 cells (Figure 14). This result suggested that the size and shape of the ODN1668/hexapodna might be the only factor influencing the cellular uptake no matter it was modified or not with mannose in the case of RAW264.7 cells. Therefore, all these results indicated that mannose modification could improve the immunostimulatory activity of CpG ODN in mannose receptor-positive cells. The confirmation of mannose receptor mediated endocytosis is under investigation.

B-type CpG ODNs, like CpG ODN 1668, contain a full phosphorothioate (PS) backbone with

one or more CpG dinucleotides[33]. PS backbone endows CpG ODN with high enzymatical stability against DNase and superior membrane permeability, but at the same time, PS modification increases the cytotoxicity of the ODNs[16, 17]. In contrast, natural phosphodiester DNA, especially short ones like ODNs, are enzymatically unstable and labile to nuclease degradation within the body[14]. The success of increased immunostimulatory activity by the combination of mannose modification and incorporation into nanostructured DNA would provide a suitable solution to increase the immunostimulatory activity and biological stability without increasing the cytotoxicity of CpG ODN.

Chapter 3

Development of Mannose-modified G-quadruplex Structured CpG ODN for Targeted Delivery to Antigen-presenting Cells

3.1 Introduction

The structure of GQ has been studied widely as an important component in nucleic acid nanotechnology, including for nanocarrier design in drug delivery[10]. In Chapter 1, the stability, cellular uptake, and immunostimulatory activity of CpG ODNs were successfully improved through G-quadruplex nanostructuration by the introduction of several guanines into the sequence. This technique provides a simple and economical strategy for CpG ODN delivery.

The mannose receptor (MR), which can specifically recognize saccharides, including mannose, is predominantly expressed on the surface of macrophages and dendritic cells[52]. In Chapter 2, it was established that mannose modification is a useful approach for the further enhancement of the immunostimulatory activity of the CpG ODN-loaded polypodna. Therefore, in this Chapter, I investigated whether the mannose modification could enhance the delivery and immunostimulatory activity of GQ-structured CpG ODNs.

In the parallel GQ structure, all ODNs are arranged in the same direction. This structural property gives rise to a situation where modifiers bound to the terminal of GQ structure-forming ODN come in close contact after GQ structuration, which leads to the aggregation of the modifiers. It has been reported that mannose density is an important parameter for ligand recognition by the MR[61]. Therefore, mannose modification of the GQ structure-forming CpG ODN might increase the interaction between GQ-structured CpG ODN and the MR, by increasing the efficiency of uptake by the MR.

Therefore, in this chapter, I focused on the GQ-structured CpG ODN, 1668(5′-G_5). I modified its 5′- and 3′-terminal amino-modified derivatives with mannose, and then investigated their structural properties and immunostimulatory activity.

3.2 Materials and Methods

Preparation of GQ-structured CpG ODNs

Phosphodiester ODNs were purchased from Integrated DNA Technologies, Inc. (Coralville, IA, USA). The sequences of the ODNs used are summarized in Table 5. GQ-structured CpG ODNs were prepared by annealing each ODN (0.5 mM) in 150 mM KCl solution, in accordance with the protocol described by Mohri *et al.*[6].

Synthesis of mannosylated CpG ODNs

Terminal amino-modified ODN1668 (20 nmol, 1 mM in distilled H_2O, 20 μL) was added to a

solution of Na_2CO_3-$NaHCO_3$ buffer (0.33 M, pH = 9, 60 μL) and DMSO (64 μL). Subsequently, compound **5**, whose synthesis has been described in Chapter 2 (20 μL, 0.5 M in DMSO, 40 μL) or α-D-mannopyranophenyl isothiocyanate (Toronto Research Chemicals Inc., ON, Canada) were added to the above mixture. After brief vortexing and centrifugation, the mixture was stored at room temperature overnight for further processing. The reactant was purified by using a Zeba spin desalting column (7K MWCO, Thermo Fisher Scientific Inc., USA) in accordance with the manufacturer's protocol, and then lyophilized to yield the product (white powder). For the CpG ODN modified by compound **5**, additional hydrolysis in 25% NH_3 (aq.), desalting, and lyophilization were performed to obtain the product. The product was then dissolved in distilled H_2O. The formation of mannosylated CpG ODN was confirmed by matrix-assisted laser desorption ionization-time of flight mass spectrometry (MALDI-TOF MS), on a JMS-S3000 spectrometer, JEOL Ltd., Japan. The yields were confirmed using Nanodrop 2000/2000c (Thermo Fisher Scientific Inc., USA). The mass and yield information are summarized in Table 6.

Table 5. Sequences of ODNs. All ODNs had a phosphodiester backbone. /5AmMC6/, 5′ amino modifier C6; /3AmMO/, 3′ amino modifier. The structures of the modifiers were shown in Figure 15 and Figure 17.

Name	Sequence (5′ to 3′)	Number of bases
1668(5′-G_5)	**GGG GG**T CCA TGA CGT TCC TGA TGC T	25
5′-NH_2-1668(5′-G_5)	/5AmMC6/**GGG GG**T CCA TGA CGT TCC TGA TGC T	25
1668(5′-G_5)-NH_2-3′	**GGG GG**T CCA TGA CGT TCC TGA TGC T/3AmMO/	25

Table 6. Calculated and MALDI-TOF mass data for modified CpG ODNs.

Name	Mannose motif	Calculated mass	Found (m/z)	Yield
5′-Man-1668(5′-G_5)	From chapter 2	8146.4	8150.8	> 99%
1668(5′-G_5)-Man-3′	From chapter 2	8178.3	8193.6	> 99%
1668(5′-Man, 5′-G_5)	α-D-mannopyranophenyl isothiocyanate	8197.5	8194.1	> 99%
1668(5′-G_5, 3′-Man)	α-D-mannopyranophenyl isothiocyanate	8229.5	8226.6	> 99%

Polyacrylamide gel (PAGE) electrophoresis

The formation of GQ-structured CpG ODNs was confirmed by polyacrylamide gel electrophoresis (PAGE) on a 6% gel at 200 V for 30 min at 4 ºC. DNA samples (0.1 μg) and a 20 bp DNA ladder (Takara, Tokyo, Japan) were resolved on the gel and ODNs were visualized by ethidium bromide (EtBr) (NIPPON GENE Co., Ltd., Tokyo, Japan) staining on a LAS4000 imaging system (FUJIFILM, Tokyo, Japan).

Animals

Female C57BL/6N mice (6-week-old) were purchased from Sankyo Labo Service Co., Inc. (Tokyo, Japan). All animal experiments received approval from the Animal Research Committee of the Faculty of Pharmaceutical Sciences, Tokyo University of Science.

Isolation of mouse peritoneal macrophages

Elicited macrophages were harvested from the peritoneal cavity of the C57BL/6N mice 3 days after intraperitoneal injection with 2 mL of 2.9% thioglycolate medium (Nissui Pharmaceutical Co. Ltd., Tokyo, Japan). The cells were washed with 1× phosphate-buffered saline (PBS) and suspended in RPMI 1640 (Nissui Pharmaceutical Co., Ltd.) supplemented with 10% heat-inactivated fetal bovine serum (Gibco, Thermo Fisher Scientific Inc., Waltham, MA, USA), penicillin G (100 U/mL), streptomycin (100 μg/mL), and L-glutamine (2 mmol/L) (Fujifilm Wako Pure Chemical Industries, Ltd., Japan) at 37 °C in a humidified incubator containing 5% CO_2. The cells were seeded in a 10 cm dish. After incubation for 2 h, non-adherent cells were removed by washing with culture medium, and the attached cells were considered as peritoneal macrophages and harvested for use in further experiments.

Cell culture

Mouse macrophage-like J774.1 cells were cultured in RPMI 1640 (Nissui Pharmaceutical Co., Ltd., Japan) supplemented with 10% heat-inactivated fetal bovine serum (Gibco, Thermo Fisher Scientific Inc.), penicillin G (100 U/mL), streptomycin (100 μg/mL), and L-glutamine (2 mmol/L) (FUJIFILM Wako Pure Chemical Co.) in a humidified incubator containing 5% CO_2 at 37 °C.

Determination of surface MR expression in J774.1 cells

Direct immunofluorescence for the surface MR on J774.1 cells was performed using the Alexa Fluor® 488 anti-mouse CD206 antibody (Bio-Rad Laboratories Inc., CA, USA) in accordance with

the manufacturer's protocol. Briefly, 1×10^6 J774.1 cells were washed and suspended in 90 μL cold (4ºC) PBS/BSA buffer; subsequently, cells were treated with 10 μL anti-CD206 antibody, and the mixture was incubated at 4 ºC in the dark for 1 h. Then, the cells were centrifuged (350 g, 5 min), washed with PBS/BSA, resuspended in 200 μL cold PBS, and analyzed by flow cytometry (Gallios Flow Cytometer; Beckman Coulter, Miami, FL, USA). Data were analyzed using FlowJo (version 8.8.4; Beckman Coulter).

IL-6 release from J774.1 cells and RAW264.7 cells

J774.1 cells (1×10^4 cells/well) or RAW264.7 cells (5×10^4 cells/well) were seeded into a 96-well plate and incubated at 37 ºC for 24 h before treatment. DNA samples diluted with Opti-modified Eagle's medium (Opti-MEM, Thermo Fisher Scientific Inc.) were used to treat J774.1 cells at a CpG ODN concentration of 20 nM, or RAW264.7 cells at a CpG ODN concentration of 100 nM, and the cells were incubated for further 8 h at 37 °C. The supernatant was collected and the concentration of interleukin (IL)-6 was determined using enzyme-linked immunosorbent assay (ELISA) in accordance with the manufacturer's protocol (Thermo Fisher Scientific Inc.).

TNF-α release from mouse peritoneal macrophages

Mouse peritoneal macrophages were seeded into a 96-well plate at a density of 1×10^5 cells/well and incubated for 24 h before the experiment. DNA samples diluted with Opti-MEM were used to treat the cells at an ODN1668 concentration of 0.6 μM, and the cells were incubated for a further 8 h in an atmosphere of 5% CO_2 at 37 °C. The supernatant was then collected and the concentration of tumor necrosis factor (TNF)-α was determined using enzyme-linked immunosorbent assay (ELISA) in accordance with the manufacturer's protocol (BioLegend, Inc., San Diego, CA, USA).

3.3 Results

3.3.1 Low GQ structure formation after modification with the synthesized mannose motif

The mannose motif, synthesized as described in Chapter 2, was first used for the mannose modification of GQ-structured CpG ODN (Figure 15). By mixing the terminal amino-modified CpG ODN and the mannose motif in buffer and performing hydrolysis, mannose-modified CpG ODNs were successfully synthesized and identified by MALDI-TOF mass spectrometry.

To confirm whether GQ-structured CpG ODNs could be generated after mannose modification, CpG ODNs in a solution of KCl were annealed and then resolved by PAGE (Figure 16). As described

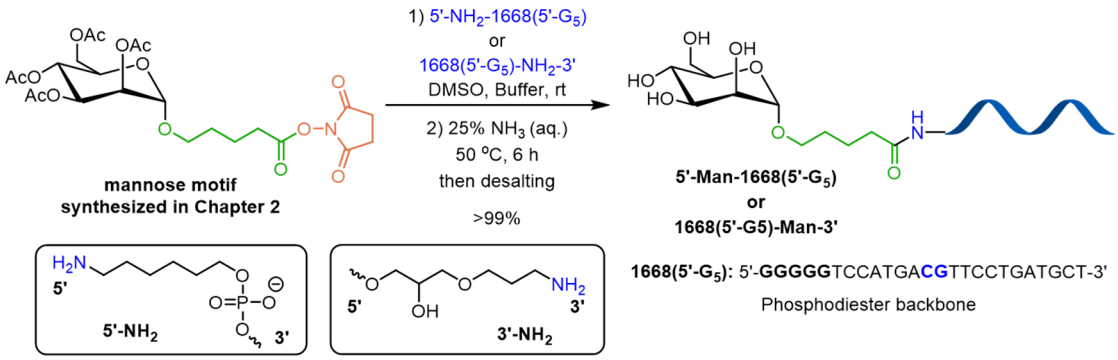

Figure 15. Synthesis of mannose-modified 1668(5′-G_5) using the mannose motif synthesized as described in Chapter 2.

in Chapter 1, 1668(5′-G_5) formed a dimeric GQ structure. The 5′-end amino-modified 1668(5′-G_5) [5′-NH_2-1668(5′-G_5)], 1668(3′-G_5), and 3′-end amino-modified 1668(3′-G_5) [1668(5′-G_5)-NH_2-3′] formed a monomeric GQ structure. However, the ODNs modified with the mannose motif, synthesized as described in Chapter 2, 5′-Man-1668(5′-G_5) and 1668(5′-G_5)-Man-3′, resulted in a relatively low conversion of single-stranded CpG ODNs to GQ-structured CpG ODNs, irrespective of the modification site. These results could be explained as the interaction of guanines with respect to GQ structure formation was interfered by long hydrophobic alkyl chain spacer between the mannose motif and the ODNs.

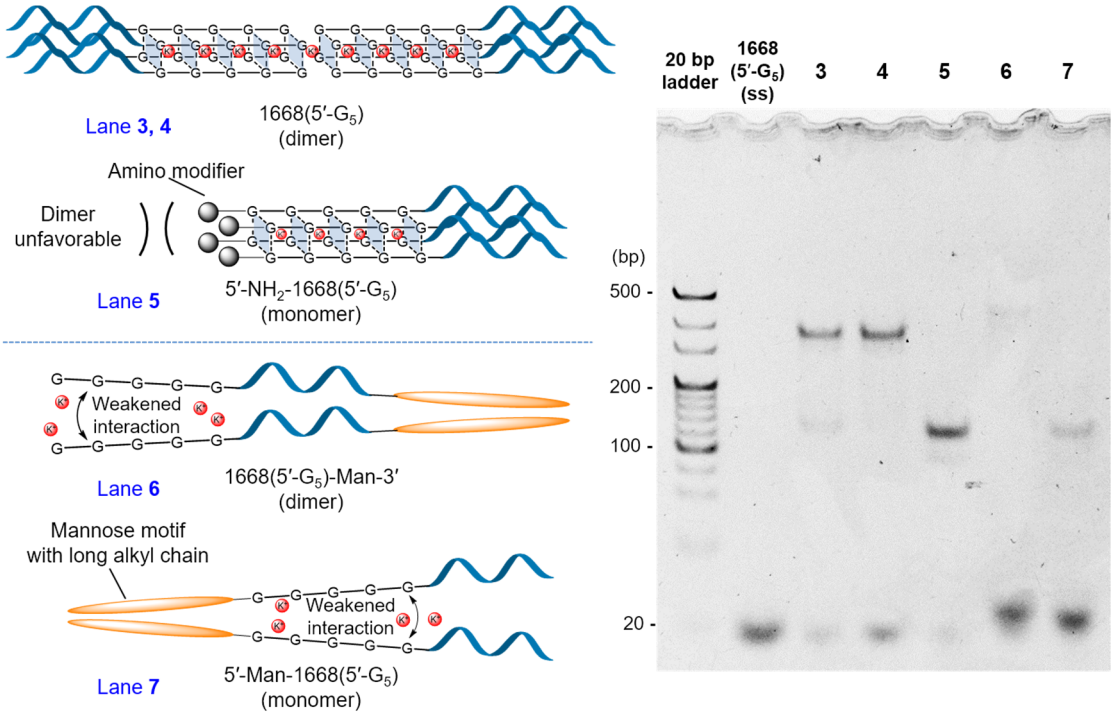

Figure 16. Confirmation of GQ structure formation after modification with the synthesized mannose motif. PAGE analysis of ODN samples. Lane 1, 20 bp ladder; lane 2, 1668(5′-G_5) annealed in distilled H_2O; lane 3 and 4, 1668(5′-G_5); lane 5, 5′-NH_2-1668(5′-G_5); lane 6, 1668(5′-G_5)-Man-3′; lane 7, 5′-Man-1668(5′-G_5).

3.3.2 GQ structure formation after modification with a mannose motif with a shorter linker

In a previous study, the synthesis of mannosylated CpG ODNs was achieved by modification of the 3′-end amino group of the CpG ODNs with α-mannopyranophenyl isocyanate[56]. This mannose motif has a shorter linker than the mannose motif synthesized in Chapter 2. Therefore, I synthesized a mannose-modified CpG ODN using this reagent (Figure 17).

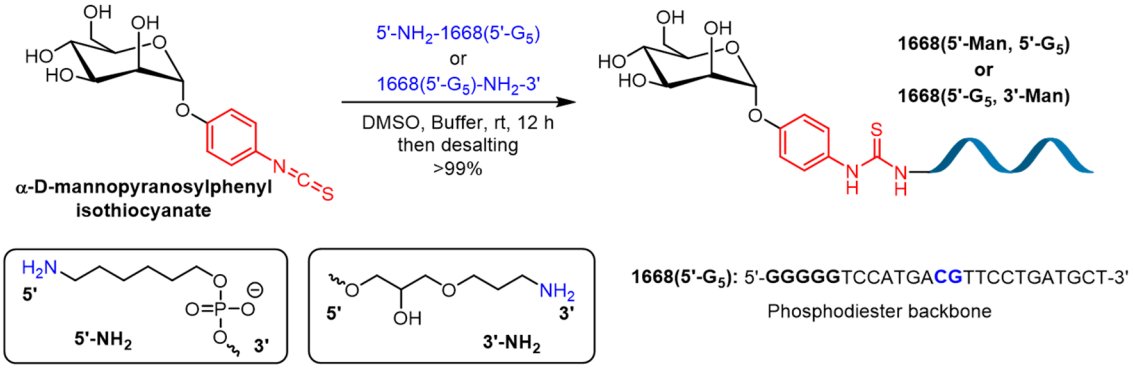

Figure 17. Synthesis of 5′- or 3′- end mannose modified 1668(5′-G$_5$) using α-D-mannopyranophenyl isothiocyanate.

Mannose-modified CpG ODNs were annealed in a solution of 150 mM KCl and were separated by PAGE. Both mannose-modified 1668(5′-G$_5$) [1668(5′-Man, 5′-G$_5$)] and mannose-modified 1668(3′-G$_5$) [1668(5′-G$_5$, 3′-Man)] were found to form GQ structures. The migration distances of these mannose-modified CpG ODNs were slightly shorter than those of unmodified CpG ODNs (Figure 18).

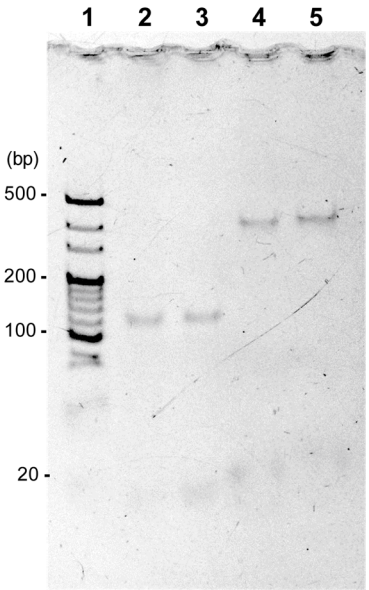

Figure 18. GQ structure formation after modification with α-D-mannopyranophenyl isothiocyanate. PAGE analysis. Lane 1, 20 bp ladder; lane 2, 5′-NH$_2$-1668(5′-G$_5$); lane 3, 1668(5′-Man, 5′-G$_5$); lane 4, 1668(5′-G$_5$)-NH$_2$-3′; lane 5, 1668(5′-G$_5$, 3′-Man).

3.3.3 Detection of surface MR expression in J774.1 cells

Prior to the evaluation of the immunostimulatory activity, the surface expression of MRs on mouse macrophage-like J774.1 cells was examined. FACS analysis revealed that almost all J774.1 cells expressed MRs on their surface (Figure 19).

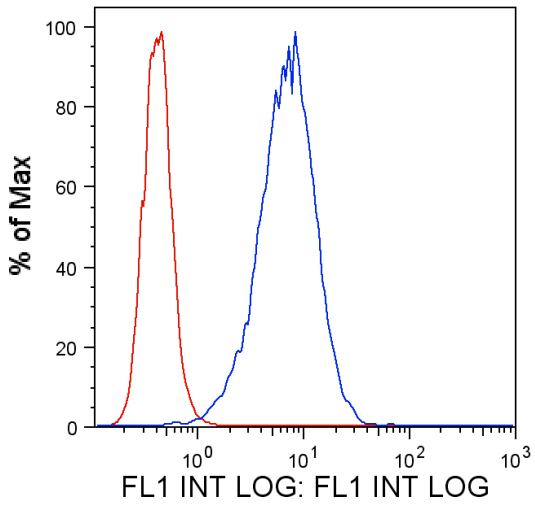

Figure 19. Surface expression of mannose receptor. J774.1 cells were labeled with Alexa Fluor 488-anti CD206 antibody. The red line represents cells without labeling (control), and the blue line represents cells labeled (stained) by the Alexa Fluor 488-anti CD206 antibody. The cells were collected, and analyzed by flow cytometry; the analysis was performed on 1×10^4 cells.

3.3.4 IL-6 release by J774.1 or RAW264.7 cells in response to treatment with mannose-modified CpG ODNs

First, 1668(5′-G_5), 5′-NH_2-1668(5′-G_5), 1668(5′-G_5)-NH_2-3′, 1668(5′-Man, 5′-G_5), and 1668(5′-G_5, 3′-Man) containing the same amount of ODN1668 (2 pmol) were used to treat J774.1 cells. The release of IL-6 from these cells 8 h after treatment is shown in Figure 20. 1668(5′-G_5, 5′-Man) induced slightly lower IL-6 release than 5′-NH_2-1668(5′-G_5). 1668(5′-G_5, 3′-Man), i.e., the 5′-end GQ-structured, 3′-mannose modified CpG ODN induced high IL-6 release from J774.1 cells (Figure 20A).

To determine whether the mannose-MR interaction is crucial for the enhancement of immunostimulatory activity, the same experiments were performed in mouse macrophage-like RAW264.7 cells, which have inherently low expression of the MR. No significant difference in IL-6 release was detected after mannose modification relative to that observed before mannose addition (Figure 20B).

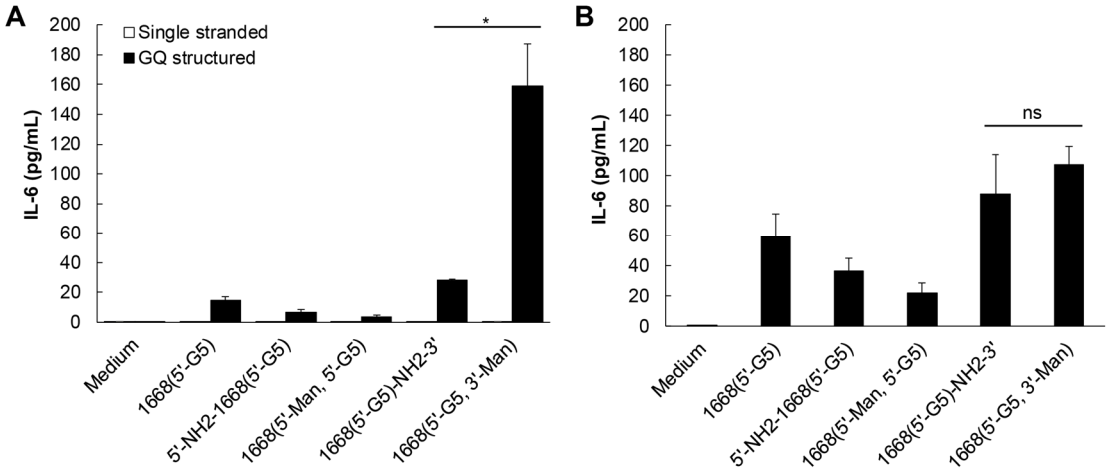

Figure 20. Enhanced immune activity of GQ structured CpG ODNs after mannose modification. (**A**) J774.1 cells or (**B**) RAW264.7 cells were treated with 1668(5′-G_5) and its derivatives. The concentration of released IL-6 was measured. The filled bars (■) represent single-stranded ODNs and hollow bars (□) represent GQ-structured ODNs. The results are expressed as the mean ± S.D. (n = 4). **p* < 0.05 by two-tailed unpaired Student's *t*-test; ns, not significant.

3.3.5 TNF-α release from mouse peritoneal macrophages after treatment of mannose-modified CpG ODNs

To test the applicability of the mannose-modified CpG ODNs, mouse peritoneal macrophages, which express the MR on their surface, were used for evaluation. Preliminary studies showed that CpG ODNs induced almost no release of IL-6 from peritoneal macrophages. Therefore, TNF-α was selected as an indicator of the immunostimulatory activity. The result suggested that mannose modification of GQ-structured CpG ODNs increased TNF-α release (Figure 21).

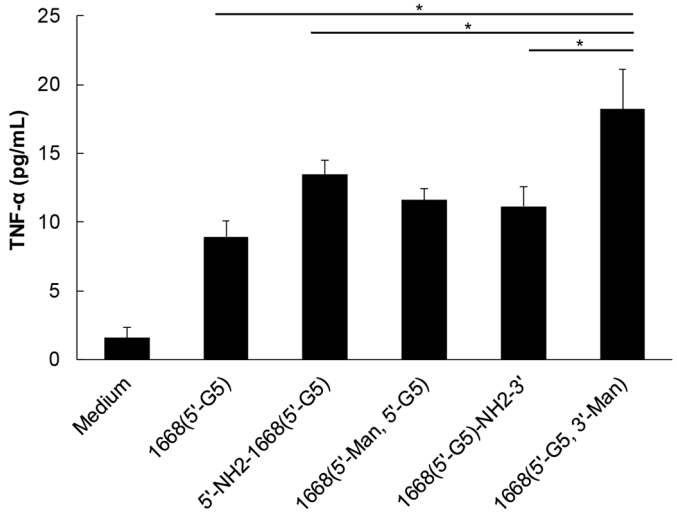

Figure 21. Increased release of TNF-α in response to GQ-structured CpG ODNs from mouse peritoneal macrophages after mannose modification. Mouse peritoneal macrophages were treated with 1668(5′-G_5) and its derivatives. The concentration of the released TNF-α was measured. The results are expressed as mean ± S.D. (n = 4). **p* < 0.05 by two-tailed unpaired Student's *t*-test.

3.4 Discussion

Ligand-receptor mediated drug delivery has been regarded as an active targeting method in DDS studies. This can be achieved by the selecting a combination of a receptor that is expressed on the target cells and a high-affinity ligand that selectively binds to the receptor[49]. The modification of nanocarriers with targeting ligands may increase their usefulness in drug delivery because the cellular uptake of nanocarriers by immune cells, the target cells for immunostimulatory nucleic acids, including CpG ODN, is dependent on the concentration and structures of the nanocarriers. In Chapter 2, it was shown that higher cytokine release was achieved with CpG ODN-loaded polypodna after mannose modification. In Chapter 1, the stability, delivery, and immunostimulatory activity of CpG ODNs was shown to be improved in response to GQ structure formation. In a parallel GQ structure, all the 5′- or 3′-ends of the ODNs are located on the same side. Given that mannose density is important for ligand recognition by the MR[61], the GQ structure formation in mannose-modified CpG ODN may be a good approach to enhance their delivery to the target immune cells and to increase the immunostimulatory activity.

As the 5′-end GQ-structured CpG ODNs form dimers, and have potentially higher mannose density than the 3′-end forms, the CpG ODN that could form the 5′-end GQ-structured CpG ODN, 1668(5′-G_5), was selected as a template for this study. In contrast with the dimeric GQ structure formation of 1668(5′-G_5), 5′-amino modified 1668(5′-G_5) formed a monomeric GQ structure (Figure 16). It was reported that the 5′-end GQ-structured ODNs were prone to thermodynamic formation of the dimer by 5′-5′ stacking, but not 5′-3′ or 3′-3′ stacking patterns[25]. This result was also consistent with the observation that an additional T, shading the GQ structure, limited the dimer formation in 5′-end GQ-structured CpG ODNs.

Low conversion efficiency from single-stranded to GQ-structured CpG ODN was obtained after modification with the mannose motif synthesized in Chapter 2 (Figure 16). This might be attributed to the following two reasons. First, this motif has a five-carbon alkyl linker , which is hydrophobic so that this conjugate has the potential to form a micelle with an inward hydrophobic chain. A recent study revealed that terminal lipid modification may lead to very rapid self-aggregation of DNA in the absence of complementary sequences[62]. In addition, the nucleotides that do not hybridize with each other contribute to DNA repulsion owing to their highly dense negative charge. Therefore, α-mannopyranophenyl isocyanate, a mannose motif with a shorter linker, was used for the modification, and all the mannose-modified ODNs successfully formed the GQ structure (Figure 18).

Single-stranded CpG ODNs hardly induced IL-6 release. Mannose modification at the 3′-end of the 5′-end GQ structured CpG ODN, i.e., 1668(5′-G_5, 3′-Man), formed a dimeric GQ structure, and

the resultant structure theoretically possessed eight mannose motifs. 1668(5′-G_5, 3′-Man) significantly increased the secretion of cytokines from the MR-positive cells, J774.1 cells and mouse peritoneal macrophages, but not from RAW264.7 cells that have relatively low MR expression (Figure 20). This suggested that mannose modification could improve the immunostimulatory activity of GQ-structured CpG ODNs in MR-positive cells through MR-mediated endocytosis. The slightly higher immunostimulatory activity of amino-modified GQ-structured CpG ODNs could be explained by the terminal modification-induced increase in stability. However, mannose modification at the 5′-end of 5′-end GQ structured CpG ODN, i.e., 1668(5′-Man, 5′-G_5), which could form four mannose motifs in a monomeric GQ structure, suppressed the release of IL-6. There are two possible explanations for this. First, the 5′-end modification further stabilized the GQ-structured CpG ODN and made it difficult to expose the CpG motif, so that the motif had almost no interaction with TLR9 because CpG ODN coordinates with TLR9 in the single-stranded form[27, 28, 41]. Second, G-quadruplex formation resulted in a bundled 5′-end, which would result in densely packed mannose motifs in the case of 5′-end mannose modification of 1668(5′-G_5), whereas mannose motifs modified at the 3′-end of 1668(5′-G_5) may have greater freedom of movement, thereby leading to multiple interactions with MRs. Therefore, the good balance between mannose density and freedom to interact with receptors, observed in case of 3′-end mannose modification, may be the reason for the strong immunostimulatory activity of 1668(5′-G_5, 3′-Man). This result also suggests that GQ structure formation, especially the formation of the GQ structure at the 5′-end, is suitable for the efficient delivery of CpG ODN containing a mannose modification at the 3′-end. Given the difficulty in obtaining dimeric GQ-structured CpG ODNs modified with the mannose motif as well as a fluorescent probe, a study on the cellular uptake of these mannose-modified CpG ODNs is now under investigation.

Conclusion

In this thesis, I focused on the development of simple strategies (1) to deliver the CpG ODN to APCs by nanostructuration using G-quadruplex just introducing several guanines into the sequence of CpG ODN and (2) to modify the DNA nanostructures including polypod-like structured nucleic acid and G-quadruplex structured CpG ODN by mannose to increase the delivery efficiency of CpG ODN to APCs. The detailed summaries are demonstrated below.

Chapter 1 Development of G-quadruplex Structured CpG ODN for Enhanced Stability and Immunoreactivity

The G-quadruplex (GQ) structure has potential applications in nucleic acid drug delivery because of its superior stability. Here, I added one G-tract (5 guanines) into a CpG ODN to construct a GQ structured CpG ODN with precise structural properties, increased biological stability, and efficient delivery to Toll-like receptor 9 (TLR9)-positive immune cells. A G-tract was added to phosphodiester-backboned CpG1668 at the 5′-end [1668(5′-G_5)], 3′-end [1668(3′-G_5)], or within the sequence [1668(mid-G_5)]. Circular dichroism analysis showed that all CpG ODNs with a G-tract formed parallel GQ structures, irrespective of its position. Electrophoresis showed that 1668(5′-G_5) formed a GQ dimer whereas others remained GQ monomers. GQ structured CpG ODNs induced greater TNF-α and IL-6 secretion from TLR9-positive mouse macrophage-like RAW264.7 cells than single-stranded CpG ODNs, with the highest for 1668(3′-G_5). GQ structuration increased CpG ODN uptake by RAW264.7 cells, and 1668(3′-G_5) decomposed more slowly in serum than 1668(5′-G_5). Thus, GQ formation with one G-tract is a simple and efficient strategy for CpG ODN delivery to TLR9-positive cells, and addition of a G-tract to the 3′-end is effective in obtaining monomeric GQ structured CpG ODN with high biological stability and immunostimulatory activity.

Chapter 2 Development of Mannose-modified Nanostructured DNA for Targeted Delivery of CpG ODN to Antigen Presenting Cells

In this study, I selected phosphodiester CpG ODN, ODN1668, that had the identical sequence to CpG1668 and a hexapodna, a polypodna with six pods, and newly designed a hexapodna that harbored ODN1668 or mannosylated CpG ODN (Man-ODN1668), which was synthesized by modification of the 5′-terminal of ODN1668 with a synthesized mannose motif. Mixing of ODN1668 or Man-ODN1668 with a hexapodna resulted in the formation of ODN1668/hexapodna and Man-ODN1668/hexapodna with high yield. The T_m measurement showed the modification hardly

influenced the thermal stability of hexapodna. Man-ODN1668/hexapodna induced greater TNF-α release from TLR9-positive mouse peritoneal macrophages than Man-ODN1668 or ODN1668/hexapodna. In addition, no improvement after mannose modification was detected from RAW264.7 cells which hardly expressed surface mannose receptor. These results indicate that the combination of mannose modification and incorporation into nanostructured DNA is an approach for enhancing the immunostimulatory activity of CpG ODN to mannose receptor positive antigen-presenting cells.

Chapter 3　Development of Mannose-modified G-quadruplex Structured CpG ODN for Targeted Delivery to Antigen Presenting Cells

To further expand the utilization efficiency of GQ structured CpG ODN, the mannose modification of GQ structured CpG ODN was conducted. Initially, 1668(5′-G_5) were successfully modified at 3′-end [1668(5′-G_5, 3′-Man)] and 5′-end [1668(5′-Man, 5′-G_5)] separately by the mannose motif which was synthesized in Chapter 2 but failed to form the GQ structure due to the steric hindrance and repulsion from the long hydrophobic linker. Modification by α-D-mannopyranosylphenyl isothiocyanate, a mannose motif with shorter linker, lead to a success in GQ structuration for both 5′- and 3′-end modification of 1668(5′-G_5). 1668(5′-G_5, 3′-Man) induced greater cytokine release from mannose receptor positive APCs, J774.1 cells and mouse peritoneal macrophages, but no improvement was detected from RAW264.7 cells which hardly expressed surface mannose receptor. These results suggested that the immunostimulatory activity of GQ structured CpG ODN could be further increased by mannose modification and the improvement from 3′-end modification of 5′-end GQ structured CpG ODNs indicated the balance between higher density of mannose motif and its degree of freedom to interact with receptors might be important to increase the interaction of CpG ODN with APCs.

As described above, the applicant clarified that the stability, delivery and immunostimulatory activity of CpG ODN can be improved by introduction of G-quadruplex structure instead of using other nanocarrier. In addition, mannose modification is suitable for enhancement of delivery of CpG ODN loaded nanostructures. The results in this study not only reveal the potential in simplification of delivery system for CpG ODN, but also provide useful information for antigen presenting cell-targeted strategy in practical application of CpG ODN.

List of Publications

Construction of Monomeric and Dimeric G-quadruplex Structured CpG Oligodeoxynucleotides for Enhanced Uptake and Activation in TLR9-positive Macrophages

Wenqing Liao, Mengmeng Tan, Kosuke Kusamori, Yoshinobu Takakura, Makiya Nishikawa

Submitted (under revision)

Enhanced Immunostimulatory Activity of CpG Oligodeoxynucleotide by Combination of Mannose Modification and Incorporation into Nanostructured DNA

Wenqing Liao, Sakiko Akahira, Rintaro Iwata Hara, Takeshi Wada, Kosuke Kusamori, Yoshinobu Takakura, Makiya Nishikawa

Submitted

Development of Mannose-modified G-quadruplex Structured CpG ODN for Targeted Delivery to Antigen-presenting Cells

Wenqing Liao, Kosuke Kusamori, Yoshinobu Takakura, Makiya Nishikawa

Manuscript in preparation

Other Publications

Nanostructured DNA for the delivery of therapeutic agents

Makiya Nishikawa, Mengmeng Tan, Wenqing Liao, Kosuke Kusamori

Adv. Drug Del. Rev., **147**, 29-36 (2019).

Photo-assisted Fixation of CO_2 onto Aryl Bromides Producing Aromatic Esters

Naoki Ishida, Yusuke Masuda, Wenqing Liao, and Masahiro Murakami

Chem. Lett., **48**, 1316-1318 (2019).

Buttressing Salicylaldehydes: A Multipurpose Directing Group for C(sp^3)-H Bond Activation

Akira Yada, Wenqing Liao, Yuta Sato, and Masahiro Murakami

Angew. Chem. Int. Ed., **56**, 1073-1076 (2017).

Synergistic Pd/Enamine Catalysis: A Strategy for the C−H/C−H Oxidative Coupling of Allylarenes with Unactivated Ketones

Shan Tang, Xudong Wu, Wenqing Liao, Kun Liu, Chao Liu, Sanzhong Luo, Aiwen Lei

Org. Lett., **16**, 3584-3587 (2014).

Revealing the metal-like behavior of iodine: an iodide-catalysed radical oxidative alkenylation

Shan Tang, Yong Wu, Wenqing Liao, Ruopeng Bai, Chao Liu, Aiwen Lei

Chem. Comm., **50**, 4496-4499 (2014).

Acknowledgement

On the course of writing this dissertation till the moment of completion, there are those who contributed to this work that I would like to express my appreciations.

Firstly, I must give my sincerest, respectful gratitude to my supervisor Prof. Dr. Yoshinobu Takakura, Department of Biopharmaceutics and Drug Metabolism, Graduate School of Pharmaceutical Sciences, Kyoto University, for leading me into the world of pharmaceutical sciences in the lecture of pharmacokinetics of which he was in charge when I was a master course student studying organic chemistry and then giving me a wonderful opportunity so that I can engage in biopharmaceutical research in Ph.D. course. His guidance and support helped me in conducting research and writing of this dissertation.

I would like to express my great appreciation to Prof. Dr. Makiya Nishikawa, Laboratory of Biopharmaceutics, Faculty of Pharmaceutical Sciences, Tokyo University of Science. Because I conducted all my researches as a special research student in Laboratory of Biopharmaceutics, he endows me detailed supervisions and dedicating academic help along the process of producing this dissertation. All his encouragements, insightful comments and supervision are fully helpful and essential for my Ph.D. course. I also would like to express my sincere gratitude to Assistant Prof. Dr. Kosuke Kusamori in Laboratory of Biopharmaceutics for his daily helpful suggestions, directions and encouragement.

I would like to express my great appreciation to Prof. Dr. Takeshi Wada, Dr. Rintaro Iwata Hara (Tokyo Medical and Dental University), Laboratory of Organic Chemistry, Faculty of Pharmaceutical Sciences, Tokyo University of Science, for their advice and providing me synthetic instrument in the early period of compound synthesis. Additionally, I would like to thank Dr. Kazuki Sato in Laboratory of Organic Chemistry for his help in circular dichroism analysis and mass identification.

I would like to express my sincere gratitude to all lab members in Laboratory of Biopharmaceutics, Faculty of Pharmaceutical Sciences, Tokyo University of Science, for their daily help and supports.

I should finally express my gratitude to my beloved parents who have always been helping me out of difficulties and supporting without a word of complaint. I also want to show my great appreciation to my wife, also one member of Nucleic Acid Group in Laboratory of Biopharmaceutics, Ms. Mengmeng Tan, for her daily discussion, concerns, supports and bringing me happiness.

References

[1] Krieg AM. Therapeutic potential of Toll-like receptor 9 activation. *Nature Reviews Drug Discovery*, **5**, 471-484 (2006).

[2] Hyer R, McGuire DK, Xing B, Jackson S, Janssen R. Safety of a two-dose investigational hepatitis B vaccine, HBsAg-1018, using a toll-like receptor 9 agonist adjuvant in adults. *Vaccine*, **36**, 2604-2611 (2018).

[3] Hanagata N. CpG oligodeoxynucleotide nanomedicines for the prophylaxis or treatment of cancers, infectious diseases, and allergies. *Int J Nanomedicine*, **12**, 515-531 (2017).

[4] Hu Q, Li H, Wang L, Gu H, Fan C. DNA Nanotechnology-Enabled Drug Delivery Systems. *Chem. Rev.*, **119**, 6459-6506 (2019).

[5] Nishikawa M, Tan M, Liao W, Kusamori K. Nanostructured DNA for the delivery of therapeutic agents. *Adv. Drug Del. Rev.*, **147**, 29-36 (2019).

[6] Mohri K, Nishikawa M, Takahashi N, Shiomi T, Matsuoka N, Ogawa K, Endo M, Hidaka K, Sugiyama H, Takahashi Y, Takakura Y. Design and Development of Nanosized DNA Assemblies in Polypod-like Structures as Efficient Vehicles for Immunostimulatory CpG Motifs to Immune Cells. *ACS Nano*, **6**, 5931-5940 (2012).

[7] Keniry MA. Quadruplex structures in nucleic acids. **56**, 123-146 (2000).

[8] Rhodes D, Lipps HJ. G-quadruplexes and their regulatory roles in biology. *Nucleic Acids Res.*, **43**, 8627-8637 (2015).

[9] Kwok CK, Merrick CJ. G-Quadruplexes: Prediction, Characterization, and Biological Application. *Trends Biotechnol.*, **35**, 997-1013 (2017).

[10] Mergny J-L, Sen D. DNA Quadruple Helices in Nanotechnology. *Chem. Rev.*, **119**, 6290-6325 (2019).

[11] Cozzoli L, Gjonaj L, Stuart MCA, Poolman B, Roelfes G. Responsive DNA G-quadruplex micelles. *Chem. Commun.*, **54**, 260-263 (2018).

[12] Grijalvo S, Alagia A, Gargallo R, Eritja R. Cellular uptake studies of antisense oligonucleotides using G-quadruplex-nanostructures. The effect of cationic residue on the biophysical and biological properties. *RSC Advances*, **6**, 76099-76109 (2016).

[13] Gay NJ, Symmons MF, Gangloff M, Bryant CE. Assembly and localization of Toll-like receptor signalling complexes. *Nature Reviews Immunology*, **14**, 546 (2014).

[14] Hanagata N. Structure-dependent immunostimulatory effect of CpG oligodeoxynucleotides

and their delivery system. *Int J Nanomedicine*, **7**, 2181-2195 (2012).

[15] Hoshi K, Yamazaki T, Sugiyama Y, Tsukakoshi K, Tsugawa W, Sode K, Ikebukuro K. G-Quadruplex Structure Improves the Immunostimulatory Effects of CpG Oligonucleotides. *Nucleic Acid Ther.*, **29**, 224-229 (2019).

[16] Srinivasan SK, Iversen P. Review of in vivo pharmacokinetics and toxicology of phosphorothioate oligonucleotides. **9**, 129-137 (1995).

[17] Henry SP, Bolte H, Auletta C, Kornbrust DJ. Evaluation of the toxicity of ISIS 2302, a phosphorothioate oligonucleotide, in a four-week study in cynomolgus monkeys. *Toxicology*, **120**, 145-155 (1997).

[18] Nishikawa M. Nucleic Acid Drugs and DNA-based Delivery Systems. *Drug Discov. Ther.*, **10**, 271-272 (2016).

[19] Takahashi Y, Maezawa T, Araie Y, Takahashi Y, Takakura Y, Nishikawa M. In Vitro and In Vivo Stimulation of Toll-Like Receptor 9 by CpG Oligodeoxynucleotides Incorporated Into Polypod-Like DNA Nanostructures. *J. Pharm. Sci.*, **106**, 2457-2462 (2017).

[20] Carvalho J, Queiroz JA, Cruz C. Circular Dichroism of G-Quadruplex: a Laboratory Experiment for the Study of Topology and Ligand Binding. *J. Chem. Educ.*, **94**, 1547-1551 (2017).

[21] Kypr J, Kejnovská I, Renčiuk D, Vorlíčková M. Circular dichroism and conformational polymorphism of DNA. *Nucleic Acids Res.*, **37**, 1713-1725 (2009).

[22] Mergny J-L, De Cian A, Ghelab A, Saccà B, Lacroix L. Kinetics of tetramolecular quadruplexes. *Nucleic Acids Res.*, **33**, 81-94 (2005).

[23] Lu M, Guo Q, Kallenbach NR. Structure and stability of sodium and potassium complexes of dT4G4 and dT4G4T. *Biochemistry*, **31**, 2455-2459 (1992).

[24] Pohar J, Lainscek D, Fukui R, Yamamoto C, Miyake K, Jerala R, Bencina M. Species-Specific Minimal Sequence Motif for Oligodeoxyribonucleotides Activating Mouse TLR9. *J. Immunol.*, **195**, 4396-4405 (2015).

[25] Kogut M, Kleist C, Czub J. Why do G-quadruplexes dimerize through the 5'-ends? Driving forces for G4 DNA dimerization examined in atomic detail. *PLoS Comput. Biol.*, **15**, e1007383 (2019).

[26] Harkness V RW, Avakyan N, Sleiman HF, Mittermaier AK. Mapping the energy landscapes of supramolecular assembly by thermal hysteresis. *Nature Communications*, **9**, 3152 (2018).

[27] Ohto U, Ishida H, Shibata T, Sato R, Miyake K, Shimizu T. Toll-like Receptor 9 Contains Two DNA Binding Sites that Function Cooperatively to Promote Receptor Dimerization and

Activation. *Immunity*, **48**, 649-658 e644 (2018).

[28] Rutz M, Metzger J, Gellert T, Luppa P, Lipford GB, Wagner H, Bauer S. Toll-like receptor 9 binds single-stranded CpG-DNA in a sequence- and pH-dependent manner. *Eur. J. Immunol.*, **34**, 2541-2550 (2004).

[29] Lee SW, Song MK, Baek KH, Park Y, Kim JK, Lee CH, Cheong HK, Cheong C, Sung YC. Effects of a hexameric deoxyriboguanosine run conjugation into CpG oligodeoxynucleotides on their immunostimulatory potentials. *J. Immunol.*, **165**, 3631-3639 (2000).

[30] Dalpke AH, Zimmermann S, Albrecht I, Heeg K. Phosphodiester CpG oligonucleotides as adjuvants: polyguanosine runs enhance cellular uptake and improve immunostimulative activity of phosphodiester CpG oligonucleotides in vitro and in vivo. *Immunology*, **106**, 102-112 (2002).

[31] Meng W, Yamazaki T, Nishida Y, Hanagata N. Nuclease-resistant immunostimulatory phosphodiester CpG oligodeoxynucleotides as human Toll-like receptor 9 agonists. *BMC Biotechnol.*, **11**, 88 (2011).

[32] Gürsel M, Verthelyi D, Gürsel I, Ishii KJ, Klinman DM. Differential and competitive activation of human immune cells by distinct classes of CpG oligodeoxynucleotide. *J. Leukoc. Biol.*, **71**, 813-820 (2002).

[33] Krieg AM. Therapeutic potential of Toll-like receptor 9 activation. *Nat. Rev. Drug Discov.*, **5**, 471-484 (2006).

[34] Krieg AM, Yi A-K, Matson S, Waldschmidt TJ, Bishop GA, Teasdale R, Koretzky GA, Klinman DM. CpG motifs in bacterial DNA trigger direct B-cell activation. *Nature*, **374**, 546-549 (1995).

[35] Akira S, Takeda K. Toll-like receptor signalling. *Nat. Rev. Immunol.*, **4**, 499-511 (2004).

[36] Murad YM, Clay TM. CpG Oligodeoxynucleotides as TLR9 Agonists. *Biodrugs*, **23**, 361-375 (2009).

[37] Scheiermann J, Klinman DM. Clinical evaluation of CpG oligonucleotides as adjuvants for vaccines targeting infectious diseases and cancer. *Vaccine*, **32**, 6377-6389 (2014).

[38] Klinman DM. Recent progress concerning CpG DNA and its use as a vaccine adjuvant AU - Shirota, Hidekazu. *Expert Review of Vaccines*, **13**, 299-312 (2014).

[39] Campbell JD. Development of the CpG Adjuvant 1018: A Case Study. *Methods in molecular biology (Clifton, N.J.)*, **1494**, 15-27 (2017).

[40] Rutz M, Metzger J, Gellert T, Luppa P, Lipford GB, Wagner H, Bauer S. Toll-like receptor 9 binds single-stranded CpG-DNA in a sequence- and pH-dependent manner. **34**, 2541-2550

(2004).

[41] Ohto U, Shibata T, Tanji H, Ishida H, Krayukhina E, Uchiyama S, Miyake K, Shimizu T. Structural basis of CpG and inhibitory DNA recognition by Toll-like receptor 9. *Nature*, **520**, 702-705 (2015).

[42] Hu Q, Li H, Wang L, Gu H, Fan C. DNA Nanotechnology-Enabled Drug Delivery Systems. *Chem. Rev.*, 10.1021/acs.chemrev.1027b00663 (2018).

[43] Nishikawa M, Ogawa K, Umeki Y, Mohri K, Kawasaki Y, Watanabe H, Takahashi N, Kusuki E, Takahashi R, Takahashi Y, Takakura Y. Injectable, self-gelling, biodegradable, and immunomodulatory DNA hydrogel for antigen delivery. *J. Control. Release*, **180**, 25-32 (2014).

[44] Li W, Luo L, Huang J, Wang Q, Liu J, Xiao X, Fang H, Yang X, Wang K. Self-assembled DNA nanocentipedes as multivalent vehicles for enhanced delivery of CpG oligonucleotides. *Chem. Commun.*, **53**, 5565-5568 (2017).

[45] Mohri K, Kusuki E, Ohtsuki S, Takahashi N, Endo M, Hidaka K, Sugiyama H, Takahashi Y, Takakura Y, Nishikawa M. Self-assembling DNA dendrimer for effective delivery of immunostimulatory CpG DNA to immune cells. *Biomacromolecules*, **16**, 1095-1101 (2015).

[46] Nishida Y, Ohtsuki S, Araie Y, Umeki Y, Endo M, Emura T, Hidaka K, Sugiyama H, Takahashi Y, Takakura Y, Nishikawa M. Self-assembling DNA hydrogel-based delivery of immunoinhibitory nucleic acids to immune cells. *Nanomedicine*, **12**, 123-130 (2016).

[47] Shiomi T, Tan M, Takahashi N, Endo M, Emura T, Hidaka K, Sugiyama H, Takahashi Y, Takakura Y, Nishikawa M. Atomic force microscopy analysis of orientation and bending of oligodeoxynucleotides in polypod-like structured DNA. *Nano Research*, **8**, 3764-3771 (2015).

[48] Ohtsuki S, Takahashi Y, Inoue T, Takakura Y, Nishikawa M. Reconstruction of Toll-like receptor 9-mediated responses in HEK-Blue hTLR9 cells by transfection of human macrophage scavenger receptor 1 gene. *Sci. Rep.*, **7**, 13661 (2017).

[49] Wicki A, Witzigmann D, Balasubramanian V, Huwyler J. Nanomedicine in cancer therapy: challenges, opportunities, and clinical applications. *J. Control. Release*, **200**, 138-157 (2015).

[50] van Kooyk Y, Rabinovich GA. Protein-glycan interactions in the control of innate and adaptive immune responses. *Nat. Immunol.*, **9**, 593-601 (2008).

[51] Lepenies B, Lee J, Sonkaria S. Targeting C-type lectin receptors with multivalent carbohydrate ligands. *Adv Drug Deliv Rev*, **65**, 1271-1281 (2013).

[52] Martinez-Pomares L. The mannose receptor. *J. Leukoc. Biol.*, **92**, 1177-1186 (2012).

[53] Higuchi Y, Nishikawa M, Kawakami S, Yamashita F, Hashida M. Uptake characteristics of

mannosylated and fucosylated bovine serum albumin in primary cultured rat sinusoidal endothelial cells and Kupffer cells. *Int. J. Pharm.*, **287**, 147-154 (2004).

[54] He X-Y, Liu B-Y, Wu J-L, Ai S-L, Zhuo R-X, Cheng S-X. A Dual Macrophage Targeting Nanovector for Delivery of Oligodeoxynucleotides To Overcome Cancer-Associated Immunosuppression. *ACS Applied Materials & Interfaces*, **9**, 42566-42576 (2017).

[55] Shibaguchi K, Tamura A, Terauchi M, Matsumura M, Miura H, Yui N. Mannosylated Polyrotaxanes for Increasing Cellular Uptake Efficiency in Macrophages through Receptor-Mediated Endocytosis. **24**, 439 (2019).

[56] Jung H, Yu G, Mok H. CpG oligonucleotide and α-d-mannose conjugate for efficient delivery into macrophages. *Applied Biological Chemistry*, **59**, 759-763 (2016).

[57] Kang B, Okwieka P, Schöttler S, Winzen S, Langhanki J, Mohr K, Opatz T, Mailänder V, Landfester K, Wurm FR. Carbohydrate-Based Nanocarriers Exhibiting Specific Cell Targeting with Minimum Influence from the Protein Corona. **54**, 7436-7440 (2015).

[58] Stein M, Keshav S, Harris N, Gordon S. Interleukin 4 potently enhances murine macrophage mannose receptor activity: a marker of alternative immunologic macrophage activation. *The Journal of Experimental Medicine*, **176**, 287-292 (1992).

[59] Moseman AP, Moseman EA, Schworer S, Smirnova I, Volkova T, von Andrian U, Poltorak A. Mannose receptor 1 mediates cellular uptake and endosomal delivery of CpG-motif containing oligodeoxynucleotides. *J. Immunol.*, **191**, 5615-5624 (2013).

[60] Taylor ME, Drickamer K. Structural requirements for high affinity binding of complex ligands by the macrophage mannose receptor. *The Journal of biological chemistry*, **268**, 399-404 (1993).

[61] Yeeprae W, Kawakami S, Yamashita F, Hashida M. Effect of mannose density on mannose receptor-mediated cellular uptake of mannosylated O/W emulsions by macrophages. *J. Controlled Release*, **114**, 193-201 (2006).

[62] Ohmann A, Göpfrich K, Joshi H, Thompson RF, Sobota D, Ranson NA, Aksimentiev A, Keyser UF. Controlling aggregation of cholesterol-modified DNA nanostructures. *Nucleic Acids Res.*, **47**, 11441-11451 (2019).